2025 SUMMER RESEARCH PROGRAM SYMPOSIUM

REU

(RESEARCH EXPERIENCES FOR UNDERGRADUATES)


LSU Health NEW ORLEANS
Certificate of Completion

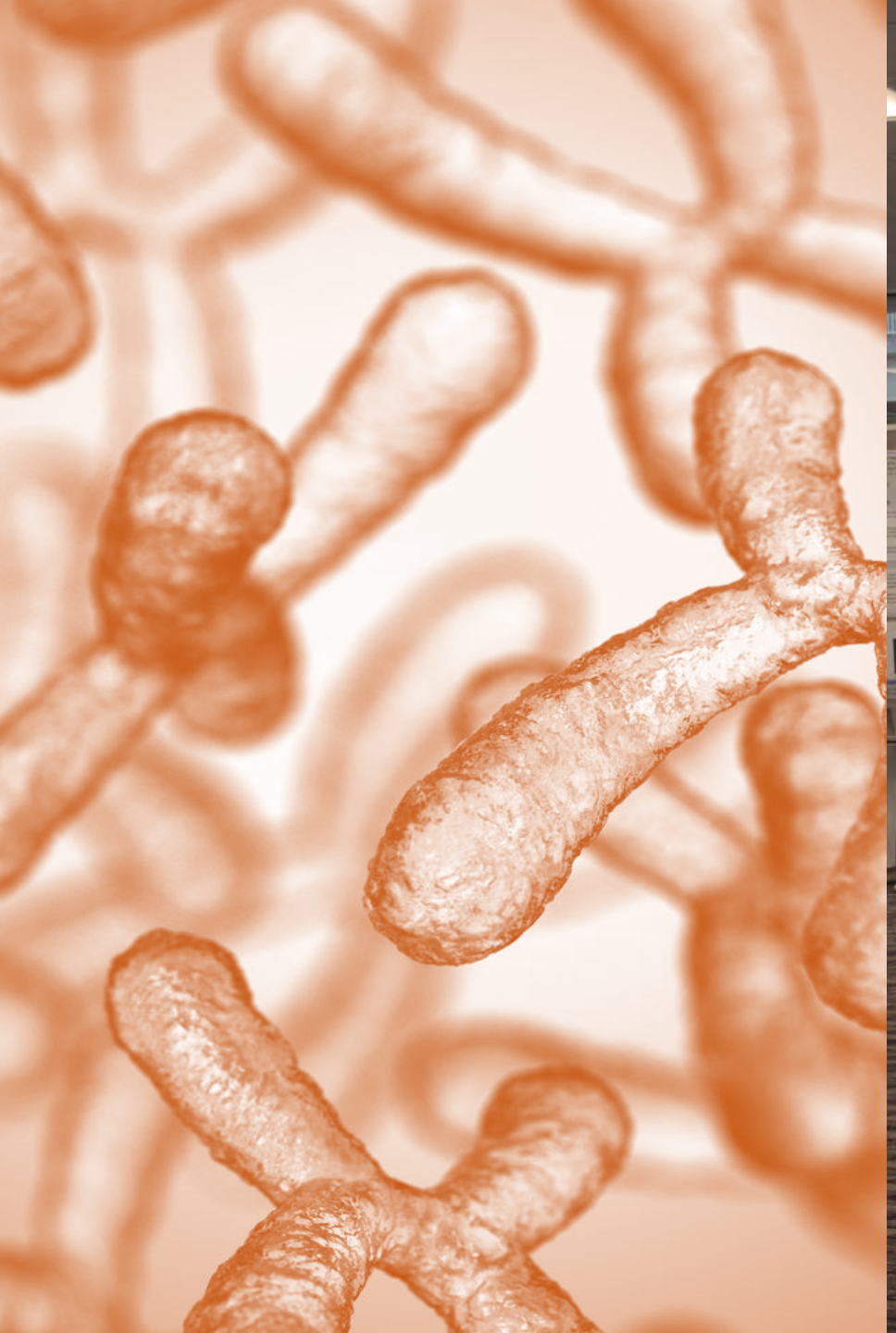

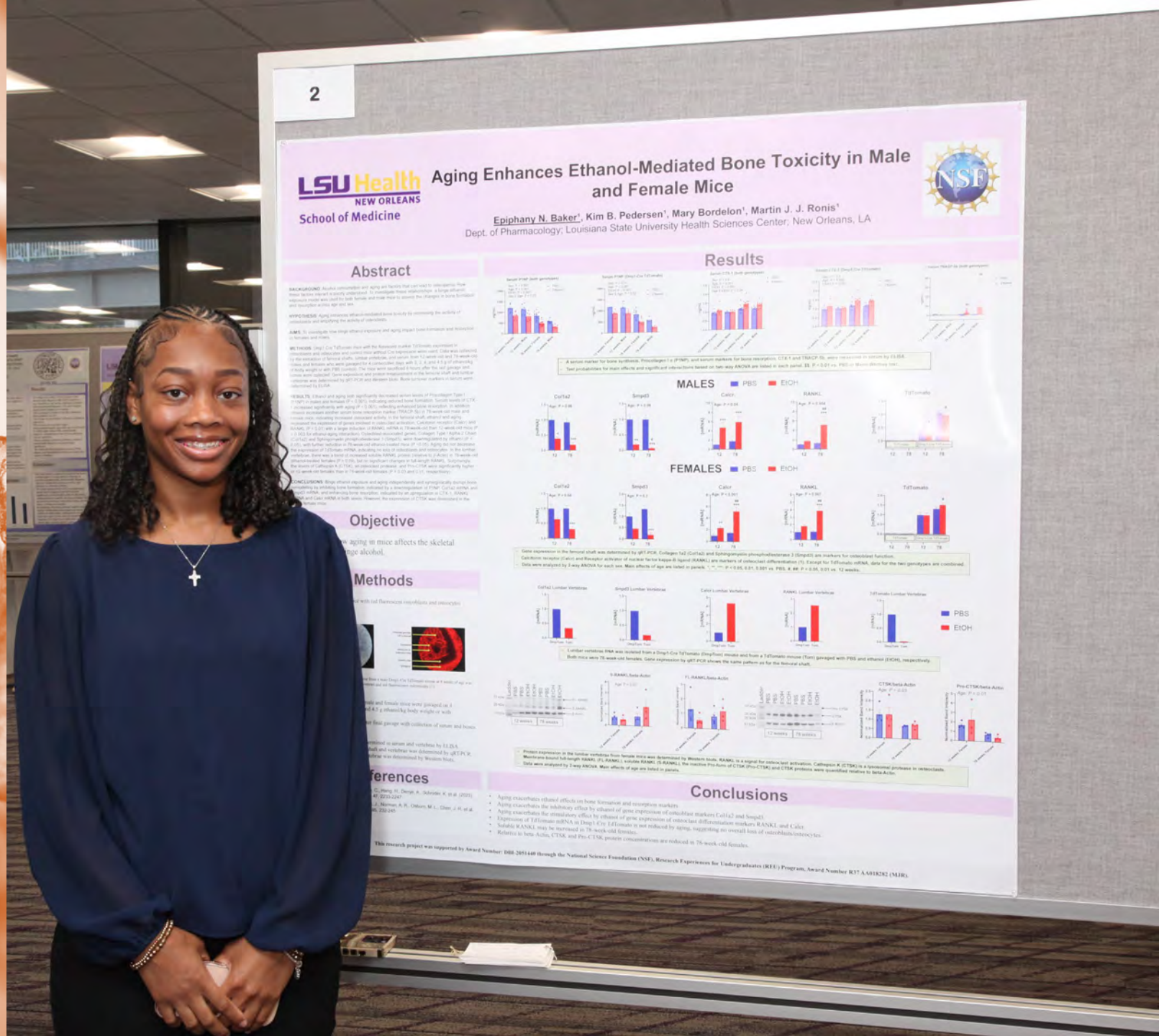
2
LSU Health NEW ORLEANS School of Medicine
Aging Enhances Ethanol-Mediated Bone Toxicity in Male and Female Mice
Epiphany N. Baker[1], Kim B. Pedersen[1], Mary Bordelon[1], Martin J. J. Ronis[1]
Dept. of Pharmacology; Louisiana State University Health Sciences Center; New Orleans, LA
NSF
Abstract
Objective
Methods
Results
MALES PBS EtOH
FEMALES PBS EtOH
Conclusions

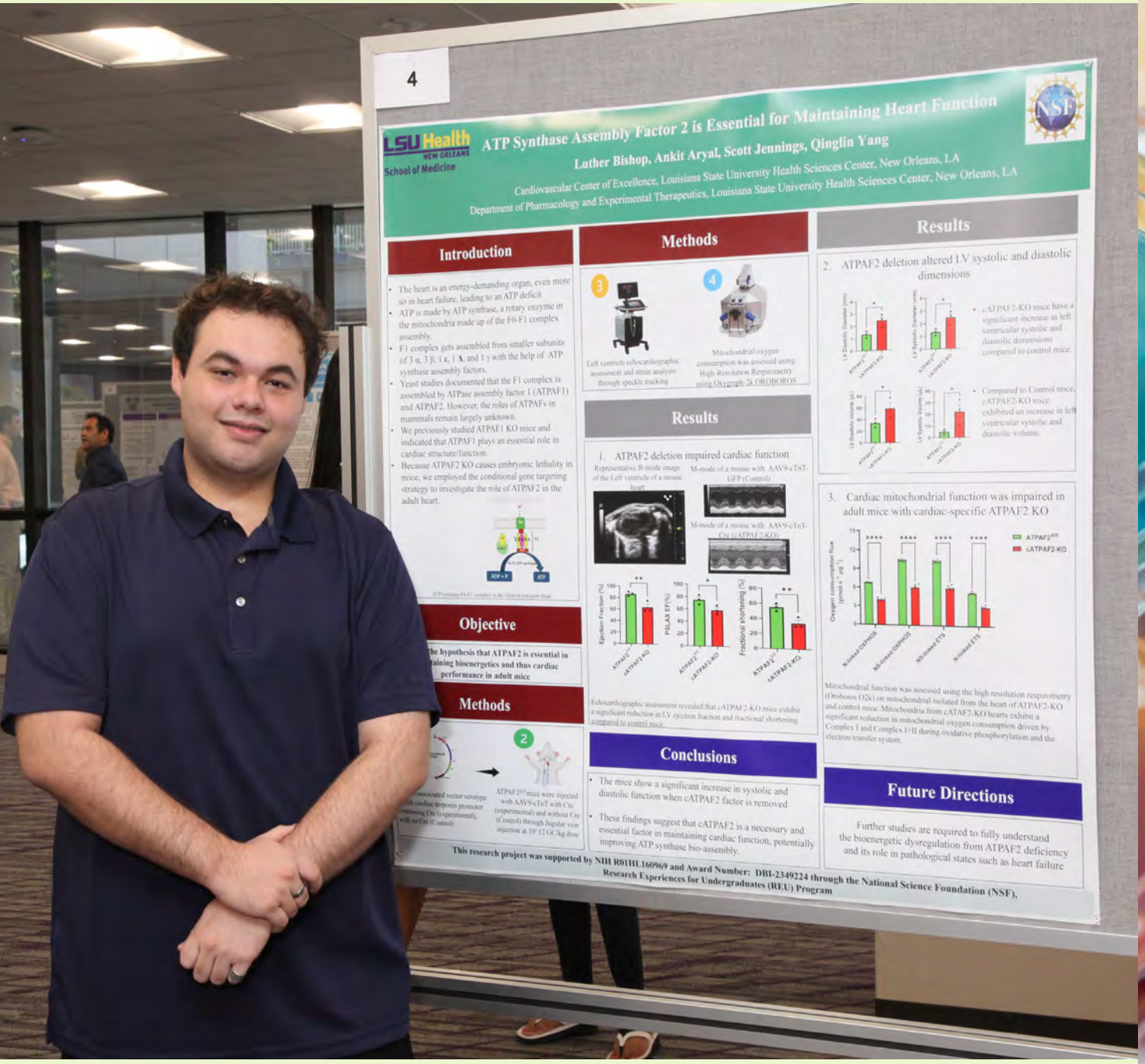
4
LSU Health NEW ORLEANS School of Medicine
ATP Synthase Assembly Factor 2 is Essential for Maintaining Heart Function
Luther Bishop, Ankit Aryal, Scott Jennings, Qinglin Yang
Cardiovascular Center of Excellence, Louisiana State University Health Sciences Center, New Orleans, LA
Department of Pharmacology and Experimental Therapeutics, Louisiana State University Health Sciences Center, New Orleans, LA
NSF
Introduction
The heart is an energy-demanding organ, even more so in heart failure, leading to an ATP deficit
ATP is made by ATP synthase, a rotary enzyme in the mitochondria made up of the F0-F1 complex assembly.
F1 complex gets assembled from smaller subunits of 3 α, 3 β, 1 ε, 1 Λ, and 1 γ with the help of ATP synthase assembly factors.
Yeast studies documented that the F1 complex is assembled by ATPase assembly factor 1 (ATPAF1) and ATPAF2. However, the roles of ATPAFs in mammals remain largely unknown.
We previously studied ATPAF1 KO mice and indicated that ATPAF1 plays an essential role in cardiac structure/function.
Because ATPAF2 KO causes embryonic lethality in mice, we employed the conditional gene targeting strategy to investigate the role of ATPAF2 in the adult heart.
Objective
The hypothesis that ATPAF2 is essential in maintaining bioenergetics and thus cardiac performance in adult mice
Methods
3
Left ventricle echocardiographic assessment and strain analysis through speckle tracking
4
Mitochondrial oxygen consumption was assessed using High-Resolution Respirometry using Oxygraph-2k OROBOROS
Results
1. ATPAF2 deletion impaired cardiac function
Representative B-mode image of the Left ventricle of a mouse heart
M-mode of a mouse with AAV9-cTnT-GFP (Control)
M-mode of a mouse with AAV9-cTnT-Cre (cATPAF2-KO)
Ejection Fraction (%)
PSLAX EF(%)
Fractional shortening (%)
Echocardiographic assessment revealed that cATPAF2-KO mice exhibit a significant reduction in LV ejection fraction and fractional shortening compared to control mice.
Conclusions
The mice show a significant increase in systolic and diastolic function when cATPAF2 factor is removed
These findings suggest that cATPAF2 is a necessary and essential factor in maintaining cardiac function, potentially improving ATP synthase bio-assembly.
Results
2. ATPAF2 deletion altered LV systolic and diastolic dimensions
LV Diastolic Diameter (mm)
LV Systolic Diameter (mm)
LV Diastolic Volume (µL)
LV Systolic Volume (µL)
cATPAF2-KO mice have a significant increase in left ventricular systolic and diastolic dimensions compared to control mice.
Compared to Control mice, cATPAF2-KO mice exhibited an increase in left ventricular systolic and diastolic volume.
3. Cardiac mitochondrial function was impaired in adult mice with cardiac-specific ATPAF2 KO
Oxygen consumption flux (pmol.s⁻¹.µg⁻¹)
ATPAF2fl/fl
cATPAF2-KO
N-linked OXPHOS
NS-linked OXPHOS
NS-linked ETS
N-linked ETS
Mitochondrial function was assessed using the high resolution respirometry (Oroboros O2k) on mitochondrial isolated from the heart of ATPAF2-KO and control mice. Mitochondria from cATAF2-KO hearts exhibit a significant reduction in mitochondrial oxygen consumption driven by Complex I and Complex I+II during oxidative phosphorylation and the electron transfer system.
Future Directions
Further studies are required to fully understand the bioenergetic dysregulation from ATPAF2 deficiency and its role in pathological states such as heart failure
This research project was supported by NIH R01HL160969 and Award Number: DBI-2349224 through the National Science Foundation (NSF), Research Experiences for Undergraduates (REU) Program

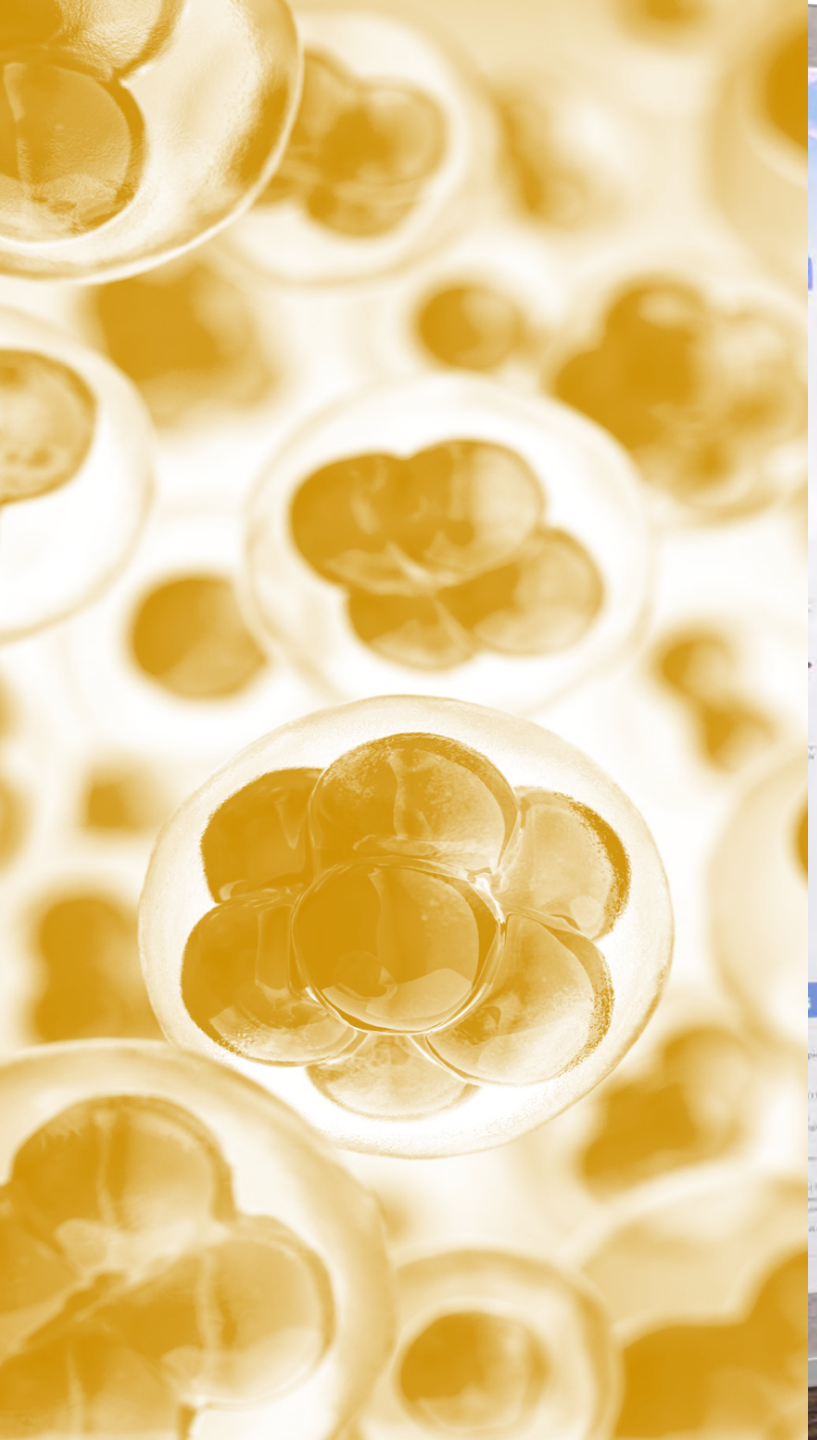

5

LSU Health NEW ORLEANS School of Medicine

An Integrative Bioinformatics Approach to Biomarker Discovery in Pancreatic Cancer

Thomas I. Blair III[1], Dr. Duaa Mohammad Alawad[2], Dr. Chindo Hicks[2]
Loyola University of New Orleans[1], Bioinformatics and Computational Medicine Program[2], Department of Genetics, LSU School of Medicine[2]

Introduction

- Pancreatic ductal adenocarcinoma (PDAC), is among the most lethal cancers with a 5-year survival rate below 10%.
- The American Cancer Society projected 66,440 new Pancreatic cancer cases and 51,750 related deaths in the U.S. in 2024.
- Clinical management of PDAC is challenged by poor response to chemotherapy and the lack of early diagnostic or prognostic biomarkers.
- This study uses integrative bioinformatics to identify diagnostic and prognostic biomarkers in PDAC from RNA-Seq and mutation data.

Objective

To discover **clinically actionable diagnostic and prognostic biomarkers** and potential **therapeutic targets** for pancreatic cancer by:

- Identifying differentially expressed genes (DEGs) between tumor vs. control, and dead vs. alive groups.
- Integrating gene expression with somatic mutation data to identify functionally relevant mutated genes.
- Performing functional enrichment and pathway analysis to identify biologically meaningful signatures.

Materials and Methods

TCGA Pancreatic Cancer Cohort (PDAC)

- RNA-Seq expression data (Tumor vs. Control; Dead vs. Alive).
- Matched somatic mutation data from whole-exome sequencing.

Table 1: Data distribution

Total	Control	Tumor		
		N= 556		
639	83	Alive	Dead	Unknown
		261	160	135

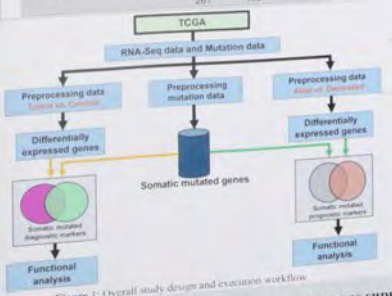

Figure 1: Overall study design and execution workflow.

Results

Tumor Vs Normal

Figure 2: Volcano plot of significantly differentially expressed (statistically mutated genes as measured by the log2FC (Tumor vs. Normal).

Table 2. List of the top 10 most highly significantly differentially expressed somatically mutated genes (tumor versus controls).

Gene	Chromosome/Position	log2FoldChange	padj	Mutation Count
KRAS	12p12.1	0.485255	1.08E-12	460
TP53	17p13.1	0.344114	0.008853	352
SMAD4	18q21.2	-0.85203	1.44E-11	107
CDKN2A	9p21.3	-1.64905	4.25E-09	100
TTN	2q31.2	-2.1241	3.47E-20	93
MUC16	19q13.2	1.697126	2.42E-09	55
ORSM6	1q42.13	0.75275	7.51E-06	54
KMT2D	12q13.12	-0.84719	1.71E-05	54
RYR1	19q13.2	-0.47291	0.013233	68
SYNE1	6q25.2	-1.59838	4.85E-13	66

Dead Vs. Alive

Figure 3: Volcano plot of significantly differentially expressed somatically mutated genes as measured by the log2FC (Dead vs. Alive).

Table 3. List of the top 10 most highly significantly differentially expressed somatically mutated genes (Dead versus Alive).

Gene	Chromosome/Position	log2FoldChange	padj	Total Mutations
KRAS	12p12.1	-0.18978	0.025645	106
TP53	17p13.1	-0.20135	0.034571	100
TTN	2q31.2	0.771291	0.00001	50
MUC16	19q13.2	1.024791	0.000131	38
RNF213	17q25	0.245449	0.028435	16
LRP1B	2q22.1-q23.2	0.578661	0.01844	14
FAT2	5q33.1	0.75216	0.000355	14
CACNA1E	1q25.3	1.09869	1.26E-05	13
ORSM6	1q42.13	0.519068	6.11E-05	13
SCN5A	3p21.3	1.162278	3.84E-10	13

Figure 4: GO enrichment analysis of differentially expressed genes between normal and tumor samples in PDAC.

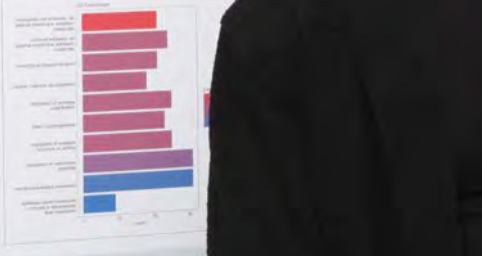

Conclusion

- Integrative analysis of gene expression and somatic mutation data revealed key diagnostic and prognostic
- including KRAS and TP53.
- Functional enrichment identified critical pathways involved in tumor progression and patient survival.
- This approach supports precision oncology and lays the foundation for developing predictive models to pr
- Future work will focus on validating candidate biomarkers experimentally and applying machine learning
- patients for clinical prioritization.

This research project was supported by Award Number: DBI-2349224 through the National Science Foundation (NSF), Research Experiences for Undergraduates (REU) Program

39

Optimizing CRISPR-Cas9 for *Rhizopus delemar*: sgRNA Screening via Bacterial On-Targeting Assays

Rayion Smith[1], Ping Wang[2]
[1]Department of Biology, Illinois Wesleyan University, Bloomington, IL, USA
[2]Department of Microbiology, Immunology and Parasitology, Louisiana State University Health Sciences Center, New Orleans, LA, USA.

LSU Health NEW ORLEANS

Introduction

The 2013 National Health Interview Survey (NHIS) estimated that 2.7 percent of U.S. adults were immunosuppressed. Recently in 2021, a NHIS study estimated that the prevalence of immunosuppressed adults in the U.S. has more than doubled, to 6.6 percent [1]. This may be due to increased used of immunosuppressive medications. The problem that arises from increases immunosuppression is severe infections caused by opportunistic fungi. A focus of this study is *Rhizopus delemar*, a zygomycetous fungus that causes mucormycosis, a rare, but aggressive and life-threatening disease. Mucormycosis presents flu-like symptoms, especially if it infects the sinuses or lungs [2]. Despite the serious infections, there is a lack of knowledge about the pathobiology of *R. delemar* due to its recalcitrant to genetic studies that could reveal molecular underpinnings of pathogenesis [3].

CRISPR-Cas9, which is a short for clustered regularly interspaced short palindromic repeats and CRISPR-associated protein 9, was adapted from the bacteria's defense system against bacteriophages, and allowed for researchers to edit the genomes of an organism's DNA [4]. We sought to use CRISPR-Cas9 gene editing as a method to analyze pathobiology at the molecular level with the goal of helping treatments for patients affected with mucormycosis.

Overall, this study tests a tool to quickly identify sgRNAs with high on-target efficiency that facilitates CRISPR-Cas9-mediated gene editing in *R. delemar*, using an all-in-one noodle construct, prior to their usage in gene edit of the fungus.

Methods

Figure 1. Cellular transformation and purification of plasmid DNA was performed to set-up a double digest. The double digest was visualized on agarose gel. Refer to figure 3.

Noodle Constructs

Figure 2. The noodle construct has sgRNA expression and targeting Cas9, and two fluorescence markers (1). A finished construct containing sgRNA C226 and sgRNA C226 target (sgRNA + PAM) (2). A construct reporter (3).

Results

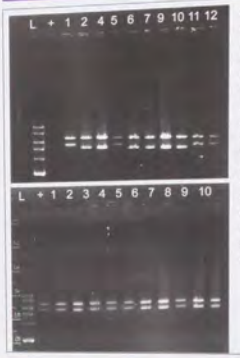

Figure 3. Top row: self-targeting occurring in 6 out of 10 C122 bacterial transformants. A smaller fragment (5.2 kb) indicates the excision of the repeater sequences resulting in reconstitution of the luciferase genes for transformants #2, #4, #6, #7, #9, and #10. Bottom row: none of the 10 C226 transformants undergo self-targeting in bacteria.

Conclusion & Future Work

The noodle construct is designed for estimating sgRNA expression and on-target efficiency through a mammalian expression system following cell culture transformation. Here we showed that the construct can also allow sgRNA expression and on-targeting during the vector cloning process in bacteria. The difference in ratios of those underwent self-targeting provide a means to quickly select sgRNAs with high on-target efficiency. Overall, this study is expected to facilitate CRISPR-Cas9-mediated gene editing and pathogenesis understanding in *R. delemar*.

In the future, the all-in-one constructs will be tested in a mammalian cell line.

Acknowledgement

I would like to thank LSUHSC for the opportunity at their summer program and assigning me to Dr. Wang, as I am grateful for his guidance. Additionally, the NSF helped make this possible with their funding.

References

1. Markson, M. J., & Lahiani, J. (2024). Prevalence of immunosuppression Among US Adults. JAMA, 331(10), 880–882. https://doi.org/10.1001/jama.2023.28019
2. (2024, May 16). Mucormycosis Basics. Mucormycosis. https://www.cdc.gov/mucormycosis/about/index.html
3. Prakash, H., Ghosh, A. K., Rudramurthy, S. M., Singh, P., Xess, I., Savio, J., ... Chakrabarti, A. (2019). A prospective multicenter study on mucormycosis in India: Epidemiology, diagnosis, and treatment. Medical Mycology, 57(4), 395–402. doi:10.1093/mmy/myy060
4. National Library of Medicine. (2021). What Are Genome Editing and CRISPR-Cas9? Medlineplus. National Library of Medicine. https://medlineplus.gov/genetics/understanding/genomicresearch/genomeediting/
5. Lin, D., Naser, S. S., Lin, Y., Mingjie, N., & Wenkun, J. A. (2024). Noodles, the all-in-one system for on-target efficiency analysis of CRISPR guide RNA. Methods, 12, 102401. doi:10.1016/j.mex.2023.102401

This research project was supported by Award Number: DBI-2349224 through the National Science Foundation (NSF), Research Experiences for Undergraduates (REU) Program

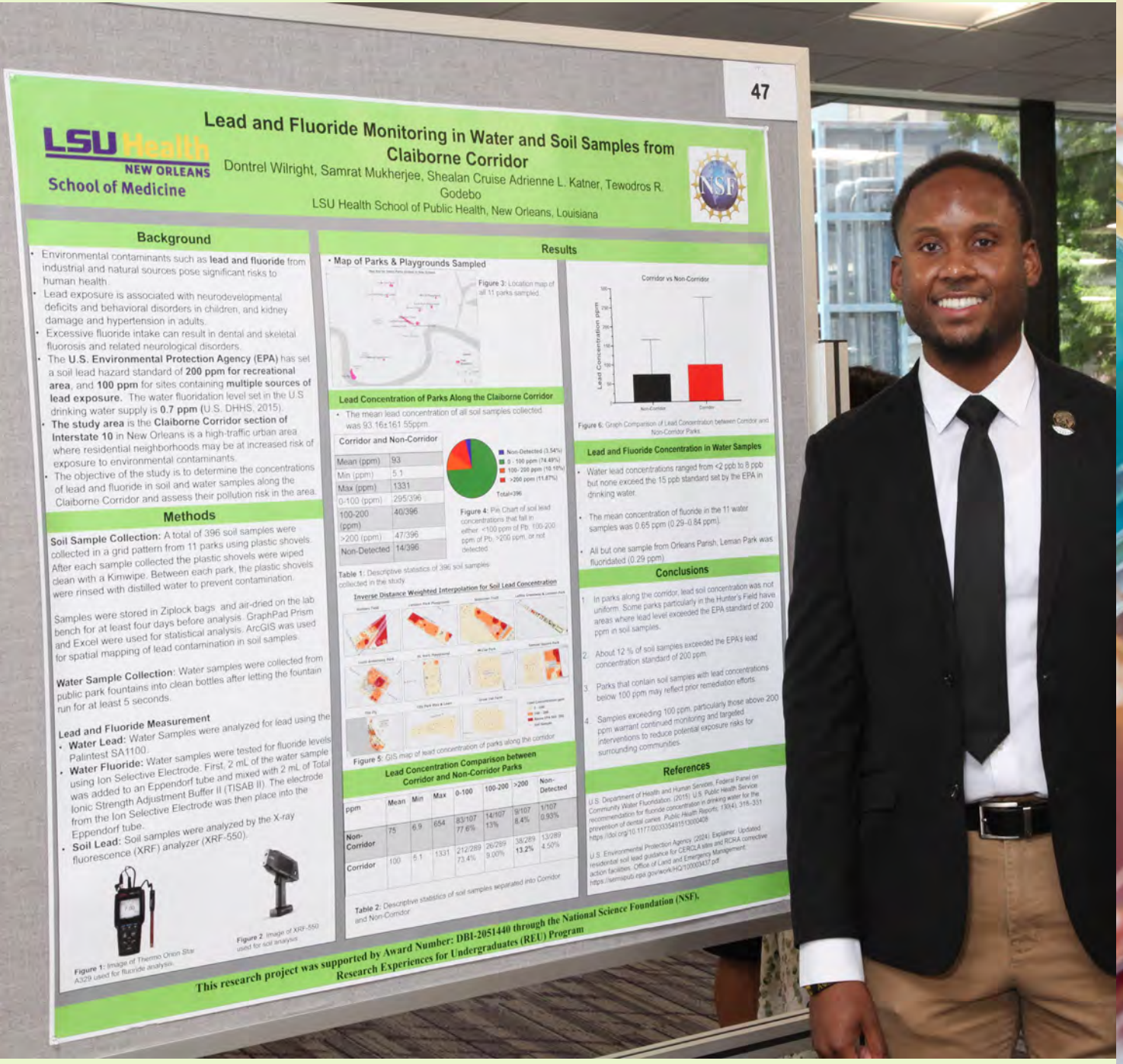
47
LSU Health NEW ORLEANS School of Medicine
Lead and Fluoride Monitoring in Water and Soil Samples from Claiborne Corridor
Dontrel Wilright, Samrat Mukherjee, Shealan Cruise Adrienne L. Katner, Tewodros R. Godebo
LSU Health School of Public Health, New Orleans, Louisiana
Background
Environmental contaminants such as lead and fluoride from industrial and natural sources pose significant risks to human health.
Lead exposure is associated with neurodevelopmental deficits and behavioral disorders in children, and kidney damage and hypertension in adults.
Excessive fluoride intake can result in dental and skeletal fluorosis and related neurological disorders.
The U.S. Environmental Protection Agency (EPA) has set a soil lead hazard standard of 200 ppm for recreational area, and 100 ppm for sites containing multiple sources of lead exposure. The water fluoridation level set in the U.S drinking water supply is 0.7 ppm (U.S. DHHS, 2015).
The study area is the Claiborne Corridor section of Interstate 10 in New Orleans is a high-traffic urban area where residential neighborhoods may be at increased risk of exposure to environmental contaminants.
The objective of the study is to determine the concentrations of lead and fluoride in soil and water samples along the Claiborne Corridor and assess their pollution risk in the area.
Methods
Soil Sample Collection: A total of 396 soil samples were collected in a grid pattern from 11 parks using plastic shovels. After each sample collected the plastic shovels were wiped clean with a Kimwipe. Between each park, the plastic shovels were rinsed with distilled water to prevent contamination.
Samples were stored in Ziplock bags and air-dried on the lab bench for at least four days before analysis. GraphPad Prism and Excel were used for statistical analysis. ArcGIS was used for spatial mapping of lead contamination in soil samples.
Water Sample Collection: Water samples were collected from public park fountains into clean bottles after letting the fountain run for at least 5 seconds.
Lead and Fluoride Measurement
Water Lead: Water Samples were analyzed for lead using the Palintest SA1100.
Water Fluoride: Water samples were tested for fluoride levels using Ion Selective Electrode. First, 2 mL of the water sample was added to an Eppendorf tube and mixed with 2 mL of Total Ionic Strength Adjustment Buffer II (TISAB II). The electrode from the Ion Selective Electrode was then place into the Eppendorf tube.
Soil Lead: Soil samples were analyzed by the X-ray fluorescence (XRF) analyzer (XRF-550).
Figure 1: Image of Thermo Orion Star A329 used for fluoride analysis.
Figure 2: Image of XRF-550 used for soil analysis
Results
Map of Parks & Playgrounds Sampled
Figure 3: Location map of all 11 parks sampled.
Lead Concentration of Parks Along the Claiborne Corridor
The mean lead concentration of all soil samples collected was 93.16±161.55ppm.
Corridor and Non-Corridor
Mean (ppm) 93
Min (ppm) 5.1
Max (ppm) 1331
0-100 (ppm) 295/396
100-200 (ppm) 40/396
>200 (ppm) 47/396
Non-Detected 14/396
Non-Detected (3.54%)
5 - 100 ppm (74.49%)
100-200 ppm (10.10%)
>200 ppm (11.87%)
Total=396
Figure 4: Pie Chart of soil lead concentrations that fall in either, <100 ppm of Pb, 100-200 ppm of Pb, >200 ppm, or not detected.
Table 1: Descriptive statistics of 396 soil samples collected in the study.
Inverse Distance Weighted Interpolation for Soil Lead Concentration
Figure 5: GIS map of lead concentration of parks along the corridor
Lead Concentration Comparison between Corridor and Non-Corridor Parks
ppm | Mean | Min | Max | 0-100 | 100-200 | >200 | Non-Detected
Non-Corridor | 75 | 6.9 | 654 | 83/107 77.6% | 14/107 13% | 9/107 8.4% | 1/107 0.93%
Corridor | 100 | 5.1 | 1331 | 212/289 73.4% | 26/289 9.00% | 38/289 13.2% | 13/289 4.50%
Table 2: Descriptive statistics of soil samples separated into Corridor and Non-Corridor
Corridor vs Non-Corridor
Lead Concentration ppm
Figure 6: Graph Comparison of Lead Concentration between Corridor and Non-Corridor Parks
Lead and Fluoride Concentration in Water Samples
Water lead concentrations ranged from <2 ppb to 8 ppb but none exceed the 15 ppb standard set by the EPA in drinking water.
The mean concentration of fluoride in the 11 water samples was 0.65 ppm (0.29 -0.84 ppm).
All but one sample from Orleans Parish, Leman Park was fluoridated (0.29 ppm)
Conclusions
1. In parks along the corridor, lead soil concentration was not uniform. Some parks particularly in the Hunter's Field have areas where lead level exceeded the EPA standard of 200 ppm in soil samples.
2. About 12 % of soil samples exceeded the EPA's lead concentration standard of 200 ppm.
3. Parks that contain soil samples with lead concentrations below 100 ppm may reflect prior remediation efforts.
4. Samples exceeding 100 ppm, particularly those above 200 ppm warrant continued monitoring and targeted interventions to reduce potential exposure risks for surrounding communities.
References
U.S. Department of Health and Human Services, Federal Panel on Community Water Fluoridation. (2015). U.S. Public Health Service recommendation for fluoride concentration in drinking water for the prevention of dental caries. Public Health Reports, 130(4), 318–331. https://doi.org/10.1177/003335491513000408
U.S. Environmental Protection Agency. (2024). Explainer: Updated residential soil lead guidance for CERCLA sites and RCRA corrective action facilities. Office of Land and Emergency Management. https://semspub.epa.gov/work/HQ/100003437.pdf
This research project was supported by Award Number: DBI-2051440 through the National Science Foundation (NSF). Research Experiences for Undergraduates (REU) Program

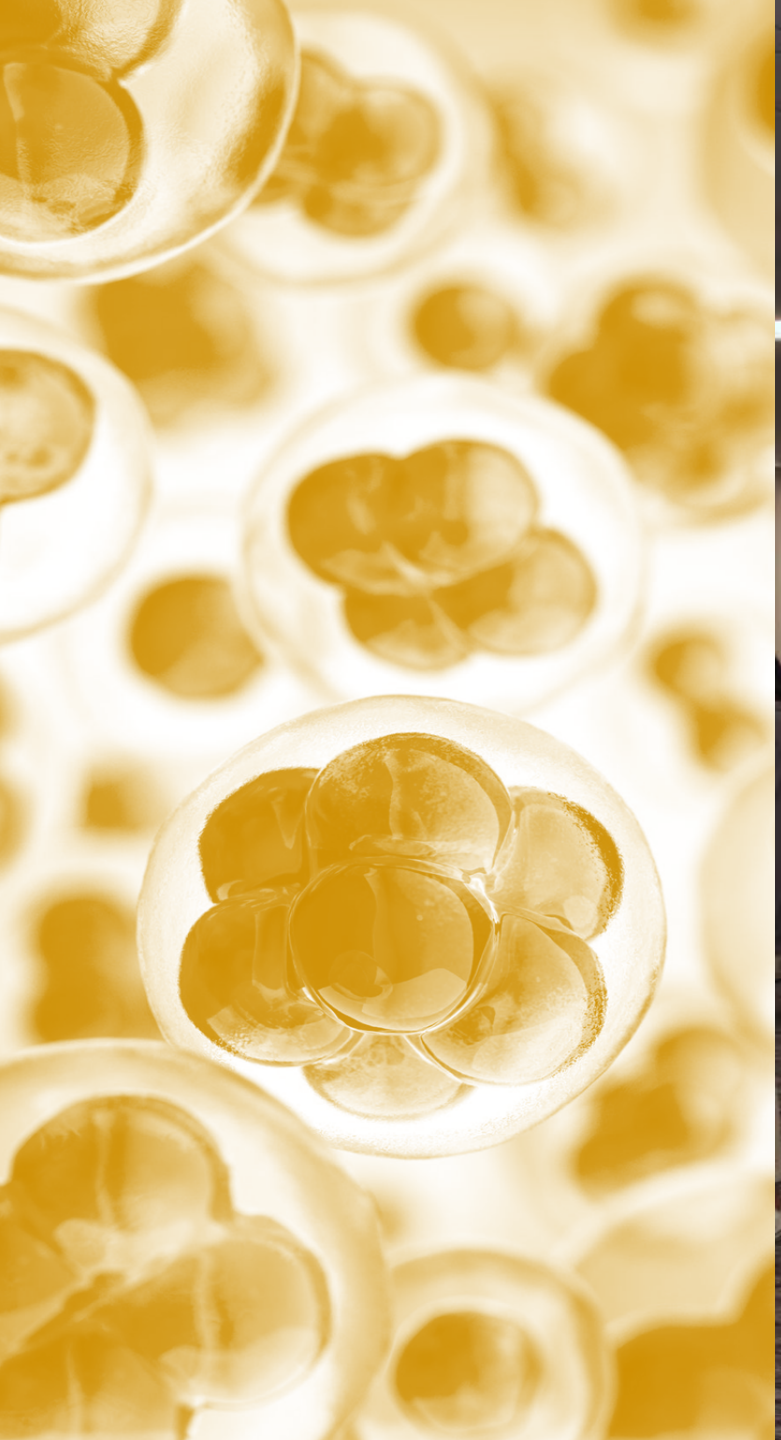

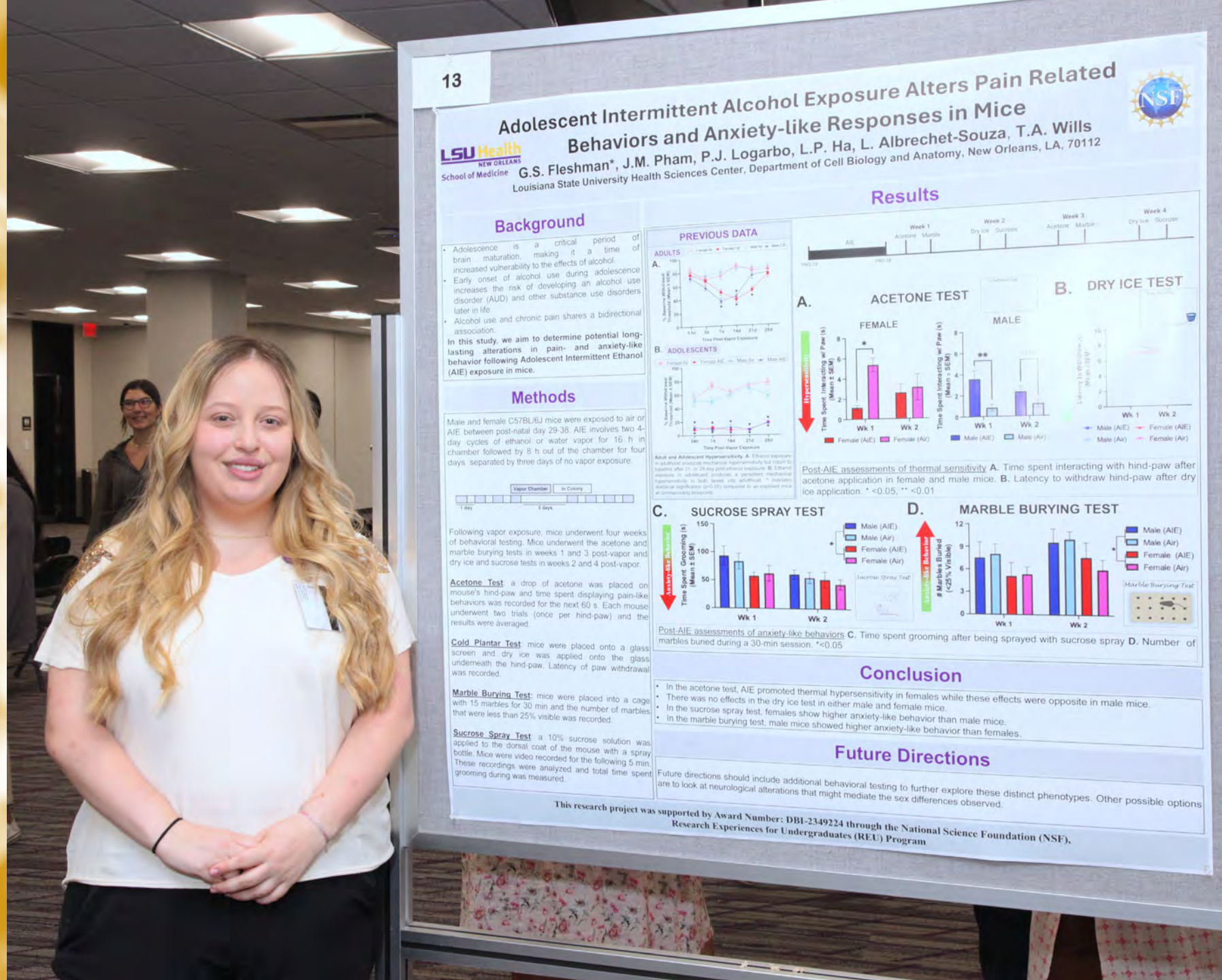

13

Adolescent Intermittent Alcohol Exposure Alters Pain Related Behaviors and Anxiety-like Responses in Mice

G.S. Fleshman*, J.M. Pham, P.J. Logarbo, L.P. Ha, L. Albrechet-Souza, T.A. Wills

Louisiana State University Health Sciences Center, Department of Cell Biology and Anatomy, New Orleans, LA, 70112

Background

- Adolescence is a critical period of brain maturation, making it a time of increased vulnerability to the effects of alcohol.
- Early onset of alcohol use during adolescence increases the risk of developing an alcohol use disorder (AUD) and other substance use disorders later in life.
- Alcohol use and chronic pain shares a bidirectional association.

In this study, we aim to determine potential long-lasting alterations in pain- and anxiety-like behavior following Adolescent Intermittent Ethanol (AIE) exposure in mice.

Methods

Male and female C57BL/6J mice were exposed to air or AIE between post-natal day 29-38. AIE involves two 4-day cycles of ethanol or water vapor for 16 h in chamber followed by 8 h out of the chamber for four days separated by three days of no vapor exposure.

Following vapor exposure, mice underwent four weeks of behavioral testing. Mice underwent the acetone and marble burying tests in weeks 1 and 3 post-vapor and dry ice and sucrose tests in weeks 2 and 4 post-vapor.

Acetone Test: a drop of acetone was placed on mouse's hind-paw and time spent displaying pain-like behaviors was recorded for the next 60 s. Each mouse underwent two trials (once per hind-paw) and the results were averaged.

Cold Plantar Test: mice were placed onto a glass screen and dry ice was applied onto the glass underneath the hind-paw. Latency of paw withdrawal was recorded.

Marble Burying Test: mice were placed into a cage with 15 marbles for 30 min and the number of marbles that were less than 25% visible was recorded.

Sucrose Spray Test: a 10% sucrose solution was applied to the dorsal coat of the mouse with a spray bottle. Mice were video recorded for the following 5 min. These recordings were analyzed and total time spent grooming during was measured.

Results

Post-AIE assessments of thermal sensitivity **A.** Time spent interacting with hind-paw after acetone application in female and male mice. **B.** Latency to withdraw hind-paw after dry ice application. * <0.05, ** <0.01

Post-AIE assessments of anxiety-like behaviors **C.** Time spent grooming after being sprayed with sucrose spray **D.** Number of marbles buried during a 30-min session. *<0.05

Conclusion

- In the acetone test, AIE promoted thermal hypersensitivity in females while these effects were opposite in male mice.
- There was no effects in the dry ice test in either male and female mice.
- In the sucrose spray test, females show higher anxiety-like behavior than male mice.
- In the marble burying test, male mice showed higher anxiety-like behavior than females.

Future Directions

Future directions should include additional behavioral testing to further explore these distinct phenotypes. Other possible options are to look at neurological alterations that might mediate the sex differences observed.

This research project was supported by Award Number: DBI-2349224 through the National Science Foundation (NSF), Research Experiences for Undergraduates (REU) Program

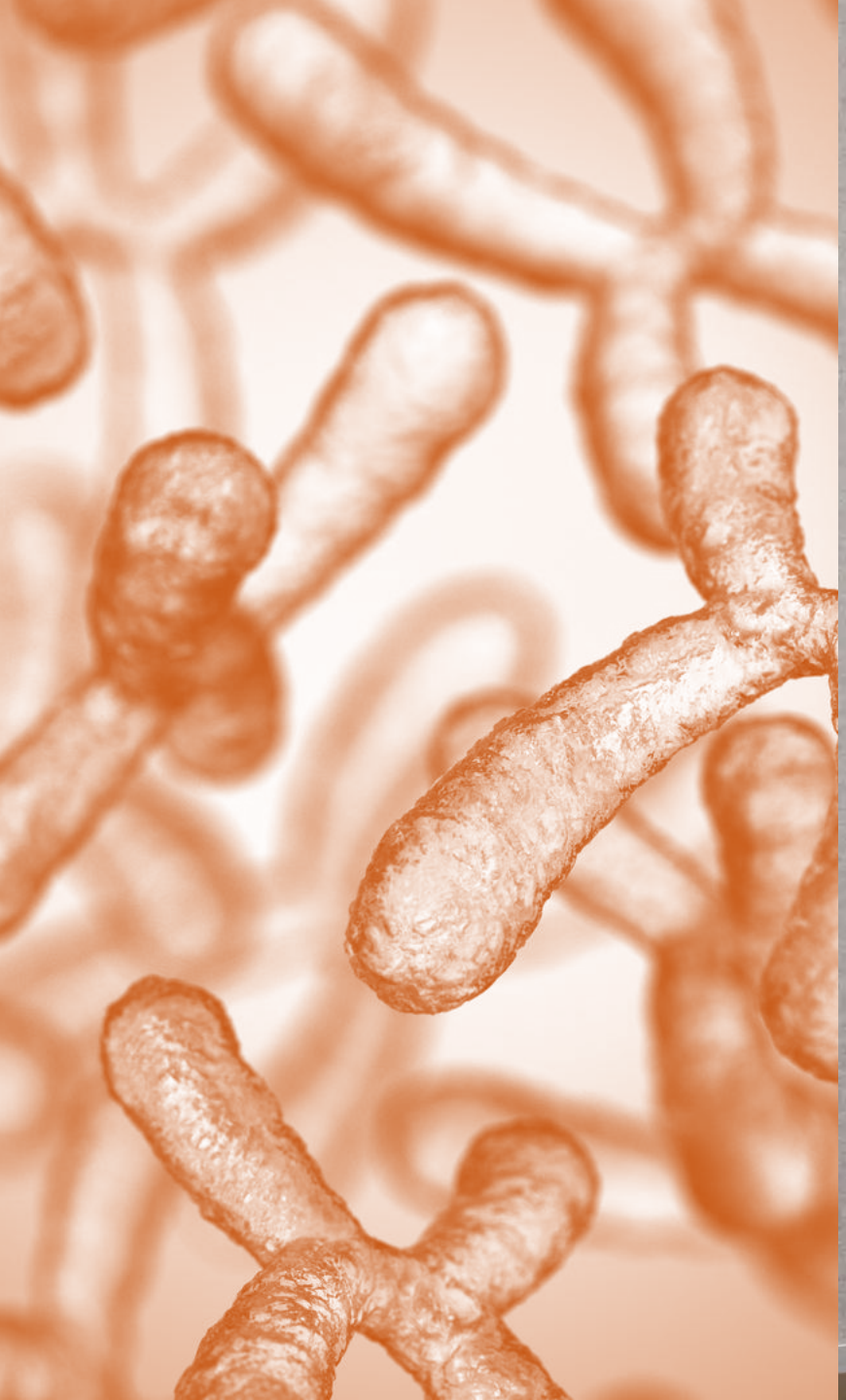

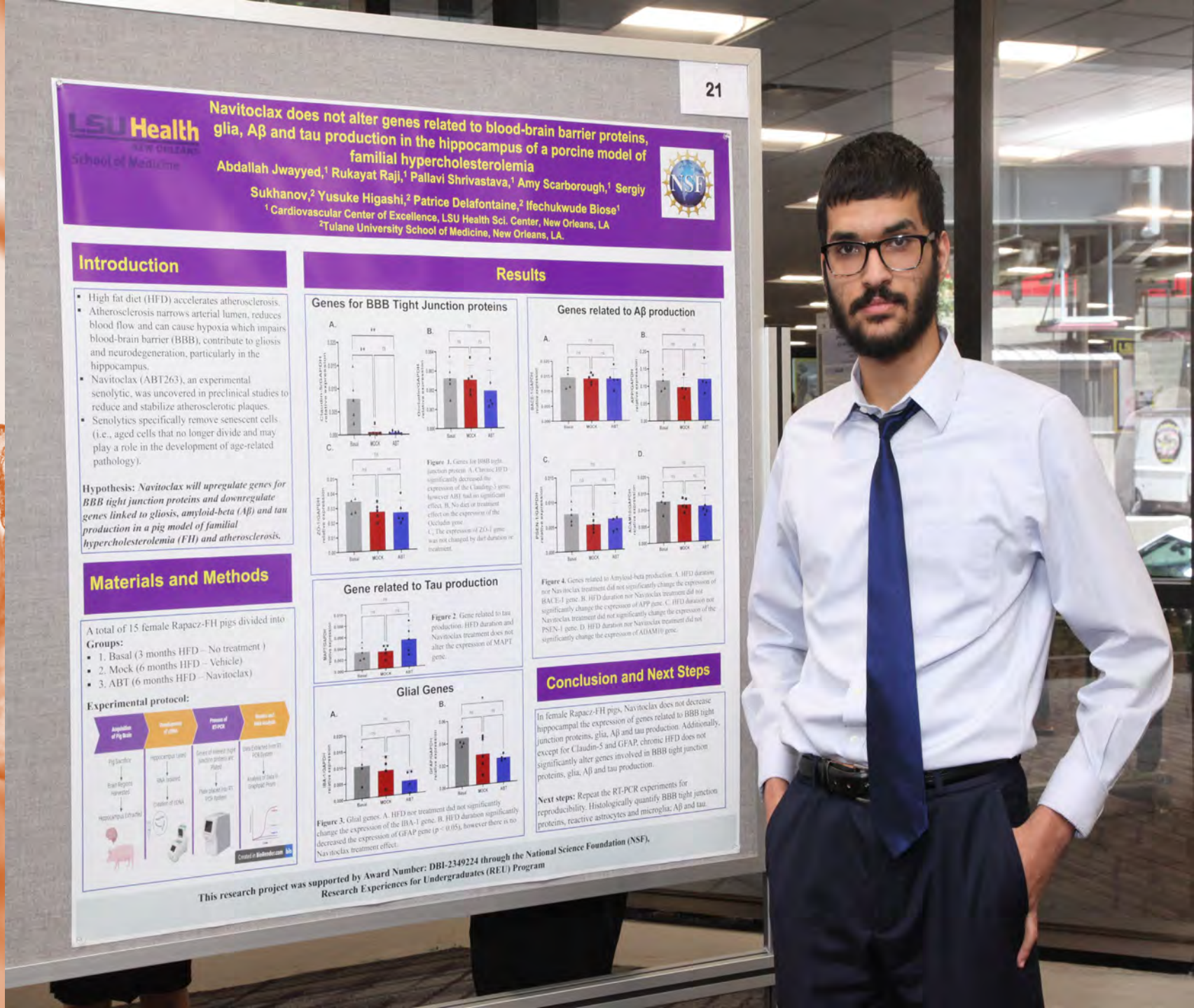

21

Navitoclax does not alter genes related to blood-brain barrier proteins, glia, Aβ and tau production in the hippocampus of a porcine model of familial hypercholesterolemia

Abdallah Jwayyed,[1] Rukayat Raji,[1] Pallavi Shrivastava,[1] Amy Scarborough,[1] Sergiy Sukhanov,[2] Yusuke Higashi,[2] Patrice Delafontaine,[2] Ifechukwude Biose[1]

[1] Cardiovascular Center of Excellence, LSU Health Sci. Center, New Orleans, LA

[2]Tulane University School of Medicine, New Orleans, LA.

Introduction

- High fat diet (HFD) accelerates atherosclerosis.
- Atherosclerosis narrows arterial lumen, reduces blood flow and can cause hypoxia which impairs blood-brain barrier (BBB), contribute to gliosis and neurodegeneration, particularly in the hippocampus.
- Navitoclax (ABT263), an experimental senolytic, was uncovered in preclinical studies to reduce and stabilize atherosclerotic plaques.
- Senolytics specifically remove senescent cells (i.e., aged cells that no longer divide and may play a role in the development of age-related pathology).

Hypothesis: ***Navitoclax will upregulate genes for BBB tight junction proteins and downregulate genes linked to gliosis, amyloid-beta (Aβ) and tau production in a pig model of familial hypercholesterolemia (FH) and atherosclerosis.***

Materials and Methods

A total of 15 female Rapacz-FH pigs divided into

Groups:

- 1. Basal (3 months HFD – No treatment)
- 2. Mock (6 months HFD – Vehicle)
- 3. ABT (6 months HFD – Navitoclax)

Experimental protocol:

Results

Genes for BBB Tight Junction proteins

Figure 1. Genes for BBB tight junction proteins. A. Chronic HFD significantly decreased the expression of the Claudin-5 gene, however ABT had no significant effect. B. No diet or treatment effect on the expression of the Occludin gene. C. The expression of ZO-1 gene was not changed by diet duration or treatment.

Gene related to Tau production

Figure 2. Gene related to tau production. HFD duration and Navitoclax treatment does not alter the expression of MAPT gene.

Glial Genes

Figure 3. Glial genes. A. HFD nor treatment did not significantly change the expression of the IBA-1 gene. B. HFD duration significantly decreased the expression of GFAP gene ($p < 0.05$), however there is no Navitoclax treatment effect.

Genes related to Aβ production

Figure 4. Genes related to Amyloid-beta production. A. HFD duration nor Navitoclax treatment did not significantly change the expression of BACE-1 gene. B. HFD duration nor Navitoclax treatment did not significantly change the expression of APP gene. C. HFD duration nor Navitoclax treatment did not significantly change the expression of the PSEN-1 gene. D. HFD duration nor Navitoclax treatment did not significantly change the expression of ADAM10 gene.

Conclusion and Next Steps

In female Rapacz-FH pigs, Navitoclax does not decrease hippocampal the expression of genes related to BBB tight junction proteins, glia, Aβ and tau production. Additionally, except for Claudin-5 and GFAP, chronic HFD does not significantly alter genes involved in BBB tight junction proteins, glia, Aβ and tau production.

Next steps: Repeat the RT-PCR experiments for reproducibility. Histologically quantify BBB tight junction proteins, reactive astrocytes and microglia; Aβ and tau.

This research project was supported by Award Number: DBI-2349224 through the National Science Foundation (NSF), Research Experiences for Undergraduates (REU) Program

25

Left atrial dysfunction is an early and transitional driver in the development of heart failure with preserved ejection fraction

Jasmine Matsuda[1], Parnia Mobasheran[1,2], Scott Jennings[1,2], Qinglin Yang[1,2]

[1]Cardiovascular Center of Excellence, Louisiana State university Health Sciences Center, New Orleans, LA 70112, USA [2]Department of Pharmacology and Experimental Therapeutics, Louisiana State university Health Sciences Center, New Orleans, LA 70112, USA 3Department of Genetics, University of Alabama at Birmingham, Birmingham, Alabama 35294, USA

Background

- Heart failure with preserved ejection fraction (HFpEF) accounts for over 50% of heart failure cases in the U.S., particularly among aging and metabolically burdened populations. Despite its prevalence, HFpEF remains poorly understood, and effective treatments are lacking.
- Recent clinical studies increasingly implicate left atrial (LA) dysfunction as a key early driver of HFpEF pathogenesis. LA plays a crucial role by acting as a reservoir during ventricular contraction.
- Impaired LA function leads to reduced LV filling or elevated filling pressures; the latter has recently proposed as a hallmark of HFpEF progression.
- It is impossible to establish the definitive LA's roles in the development and progression of HFpEF in patients. To address this, we developed a novel pre-clinical mouse model to investigate how LA plays a critical role in initiating and sustaining HFpEF.

Method

Using a fine-tip cautery pen, we applied controlled epicardial burns to the left atrial (LA) surface of 5–6-month-old male C57BL/6J mice to induce localized atrial dysfunction (AD). Burns were distributed across multiple non-overlapping regions to achieve widespread injury (Fig. 1). Mice were assigned to three groups, including sham (no injury), mild AD (3 burns), and moderate AD (5 burns). Over the following 4 weeks, we evaluated cardiac function (transthoracic echocardiography), pulmonary function (whole-body plethysmography), and exercise capacity (treadmill test) to monitor disease progression.

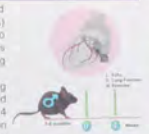

Figure 1. Experimental plan

AD causes systolic and diastolic heart function impairment

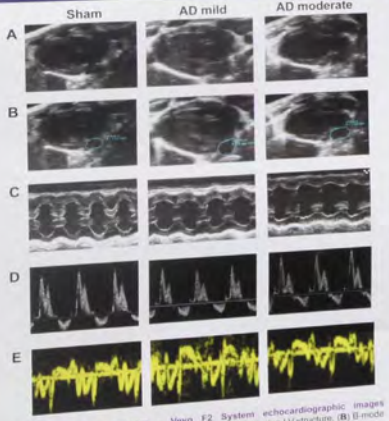

Figure 2. Echocardiogram – Vevo F2 System echocardiographic images comparing Sham and AD mice. (**A**) B-mode image showing LV structure, (**B**) B-mode image with LA area trace (d = diastolic), (**C**) M-mode image assessing LV contraction. (**D**) PW Doppler. (**E**) Tissue Doppler

Left atrial injury leads to severity-dependent ventricular functional impairment

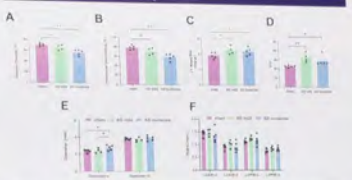

Figure 3. Echocardiography measurement of sham, mild and moderate AD. (**A-C**) LV ejection fraction (EF) and fractional shortening (FS) LV mass normalized to body weight. (**D**) E to E' ratio (**E**) LV chamber diameter, systole(s), diastolic (d) (**F**) LV wall thickness

Regional and directional LV strain analysis using Speckle tracking echocardiography

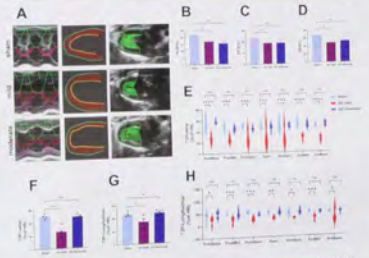

Figure 4. LV Speckle tracking echocardiography of sham, mild and moderate AD. (**A**) Schematic images of strain analysis. (**B-D**) Global longitudinal, circumferential, and radial strain. (**E**) Regional time-to-peak (T2P) of LV radial strain normalized to heart rate. (**F**) Average T2P radial across segments. (**H**) Regional T2P of LV longitudinal strain normalized to heart rate.

Left atrial structural and functional changes following graded atrial injury

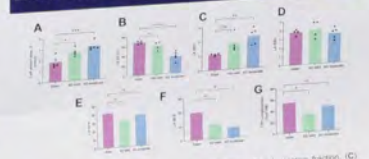

Figure 5. LA function analysis (**A**) LA area in diastole, (**B**) LA ejection fraction, (**C**) LA end-diastolic volume (EDV), (**D**) LA end-systolic volume (ESV), (**E-F**) LA circumferential (GCS) and longitudinal (GLS) strain, (**G**) time to peak of LA maximal contraction

Exercise capacity is reduced in both mild and moderate AD

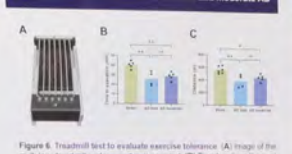

Figure 6. Treadmill test to evaluate exercise tolerance. (**A**) Image of the multi-lane treadmill system used in experiment, (**B**) Time to exhaustion and (**C**) Distance run.

Pulmonary dysfunction emerges in mild AD but not in moderate AD

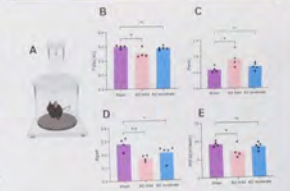

Figure 7. Lung function analysis on experimental groups. (**A**) Image of the whole-body plethysmography chamber used to assess lung function in conscious, unrestrained mice. (**B**)Tidal volume (TVb) and (**C**) Enhanced pause (Penh) (**D**) RpeF, a measure of expiratory flow, (**E**) Peak inspiratory flow (PIFb).

Conclusion and future direction

Conclusion

- Mild AD findings closely resemble the HFpEF phenotype, emphasizing LA dysfunction as a critical early and transitional driver.
- Above results provide strong evidence supporting the hypothesis that LA is a crucial hallmark in the development and progression of HFpEF.
- This highly innovative preclinical model provides a valuable platform to study the pathogenesis and pathologic mechanisms of HFpEF, explore therapeutic targets, and identify biomarkers for early detection.

Future direction

- Measuring histological changes (e.g., collagen deposit inflammation) to quantify the extent of LA dysfunction and impact on diastolic function.
- Measuring molecular markers of heart failure, such as brain natriuretic protein (BNP).
- Using catheterization to measure end systolic and end diastolic pressure to validate cardiac function changes.

References

- Khan, Muhammad Shahzeb, et al. "Left atrial function in heart failure with preserved ejection fraction: a systematic review and meta-analysis." European Journal of Heart Failure 22.3 (2020): 472-485.
- Fang, Fang, Alex Pui-Wai Lee, and Cheuk-Man Yu. "Left atrial function in heart failure with impaired and preserved ejection fraction." Current opinion in cardiology 29.5 (2014): 430-436.

This research project was supported by Award Number: DBI-2349224 through the National Science Foundation (NSF). Research Experiences for Undergraduates (REU) Program

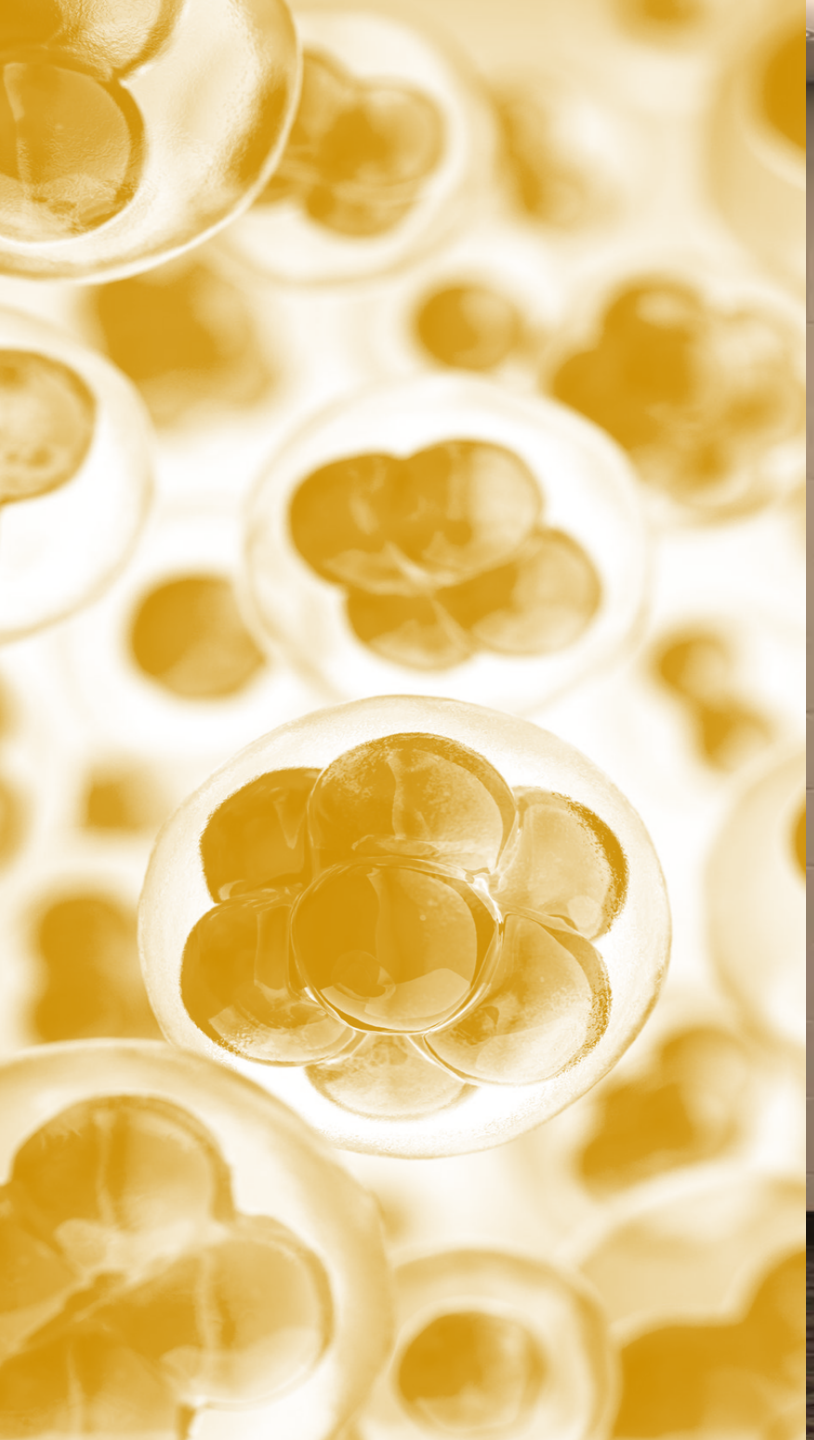

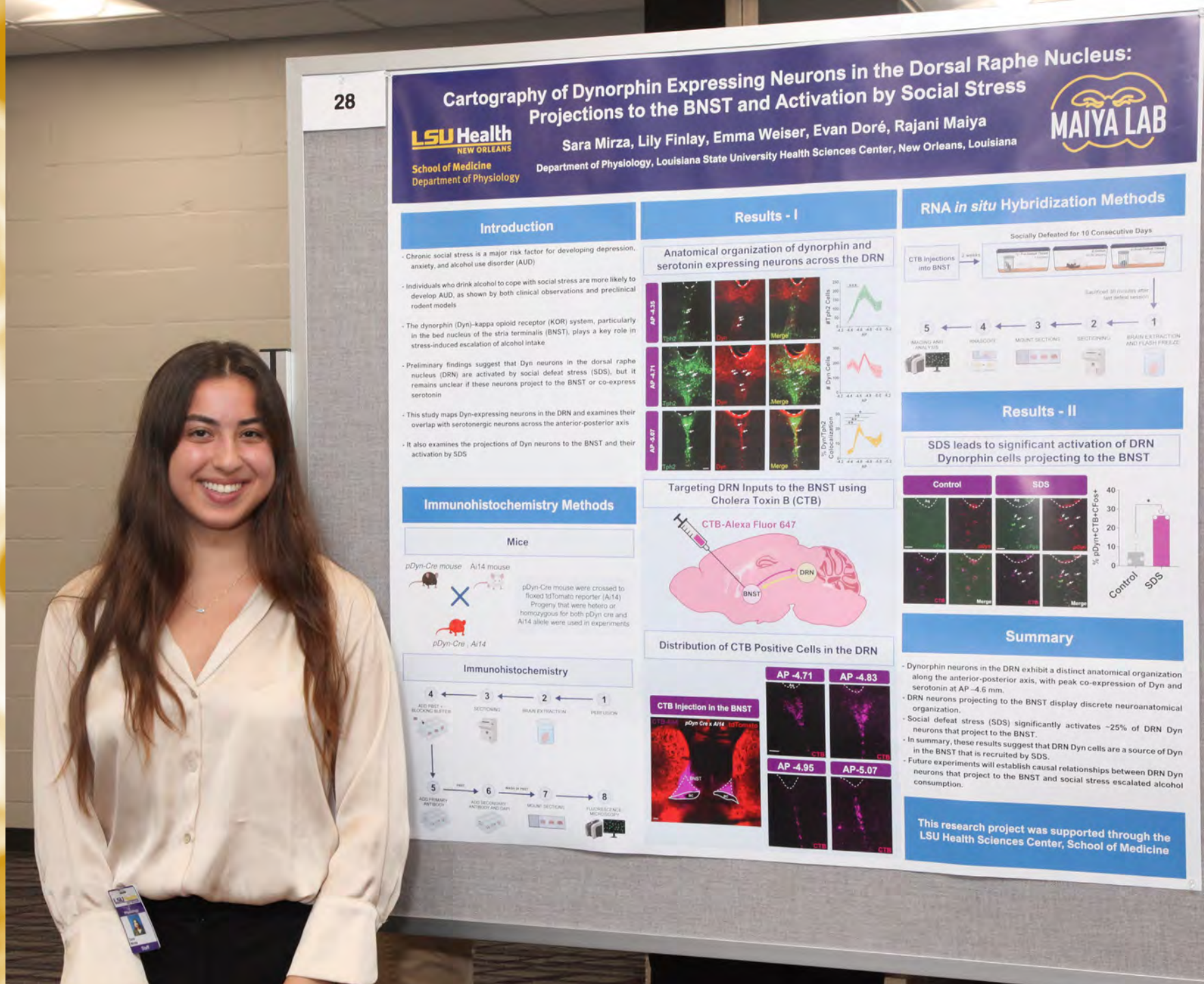

28

Cartography of Dynorphin Expressing Neurons in the Dorsal Raphe Nucleus: Projections to the BNST and Activation by Social Stress

LSU Health NEW ORLEANS
School of Medicine
Department of Physiology

Sara Mirza, Lily Finlay, Emma Weiser, Evan Doré, Rajani Maiya

Department of Physiology, Louisiana State University Health Sciences Center, New Orleans, Louisiana

MAIYA LAB

Introduction

- Chronic social stress is a major risk factor for developing depression, anxiety, and alcohol use disorder (AUD)
- Individuals who drink alcohol to cope with social stress are more likely to develop AUD, as shown by both clinical observations and preclinical rodent models
- The dynorphin (Dyn)-kappa opioid receptor (KOR) system, particularly in the bed nucleus of the stria terminalis (BNST), plays a key role in stress-induced escalation of alcohol intake
- Preliminary findings suggest that Dyn neurons in the dorsal raphe nucleus (DRN) are activated by social defeat stress (SDS), but it remains unclear if these neurons project to the BNST or co-express serotonin
- This study maps Dyn-expressing neurons in the DRN and examines their overlap with serotonergic neurons across the anterior-posterior axis
- It also examines the projections of Dyn neurons to the BNST and their activation by SDS

Immunohistochemistry Methods

Mice

pDyn-Cre mouse × Ai14 mouse → pDyn-Cre ; Ai14

pDyn-Cre mouse were crossed to floxed tdTomato reporter (Ai14) Progeny that were hetero or homozygous for both pDyn cre and Ai14 allele were used in experiments

Immunohistochemistry

Results - I

Anatomical organization of dynorphin and serotonin expressing neurons across the DRN

Targeting DRN Inputs to the BNST using Cholera Toxin B (CTB)

Distribution of CTB Positive Cells in the DRN

RNA *in situ* Hybridization Methods

Results - II

SDS leads to significant activation of DRN Dynorphin cells projecting to the BNST

Summary

- Dynorphin neurons in the DRN exhibit a distinct anatomical organization along the anterior-posterior axis, with peak co-expression of Dyn and serotonin at AP ~4.6 mm.
- DRN neurons projecting to the BNST display discrete neuroanatomical organization.
- Social defeat stress (SDS) significantly activates ~25% of DRN Dyn neurons that project to the BNST.
- In summary, these results suggest that DRN Dyn cells are a source of Dyn in the BNST that is recruited by SDS.
- Future experiments will establish causal relationships between DRN Dyn neurons that project to the BNST and social stress escalated alcohol consumption.

This research project was supported through the LSU Health Sciences Center, School of Medicine

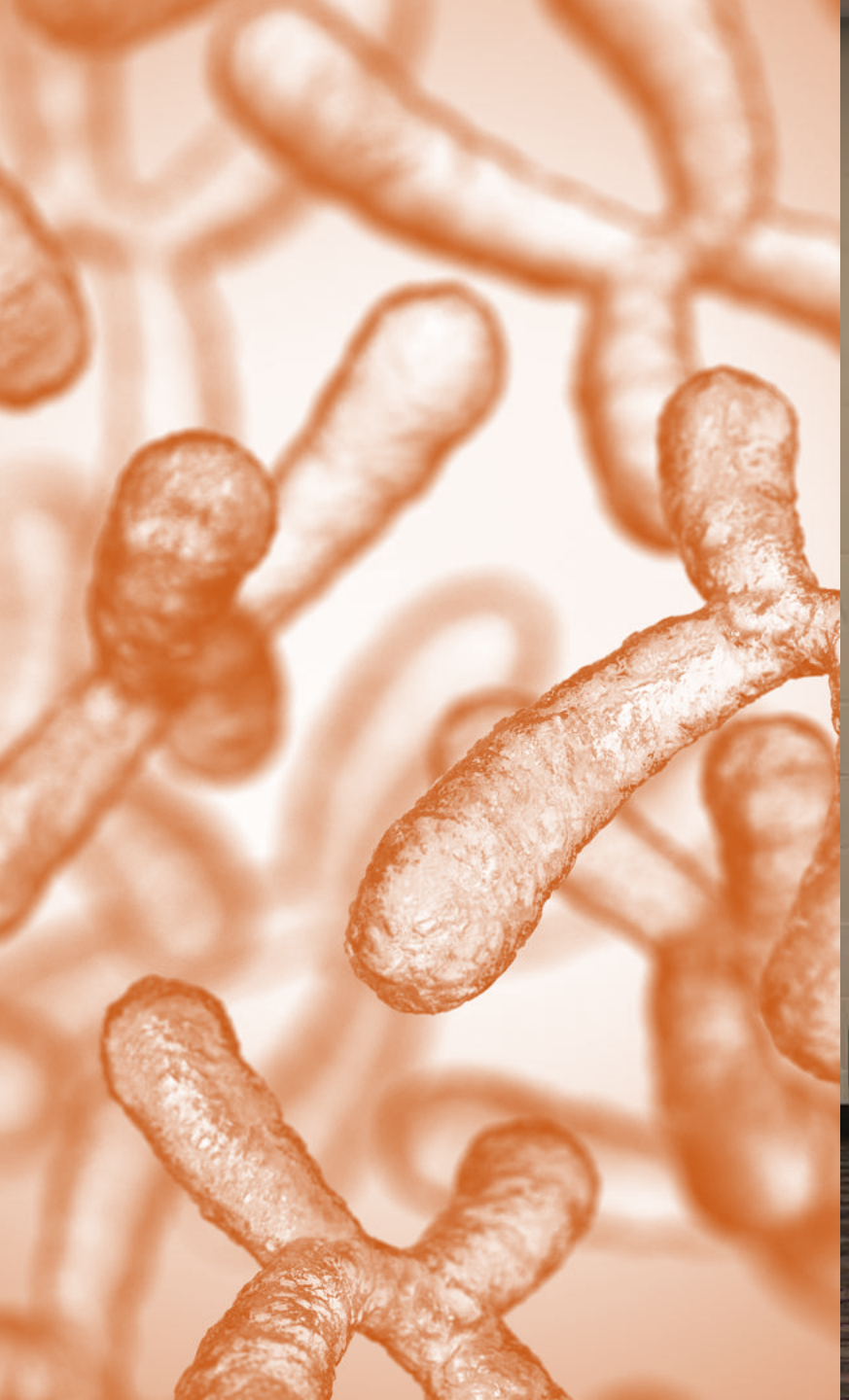

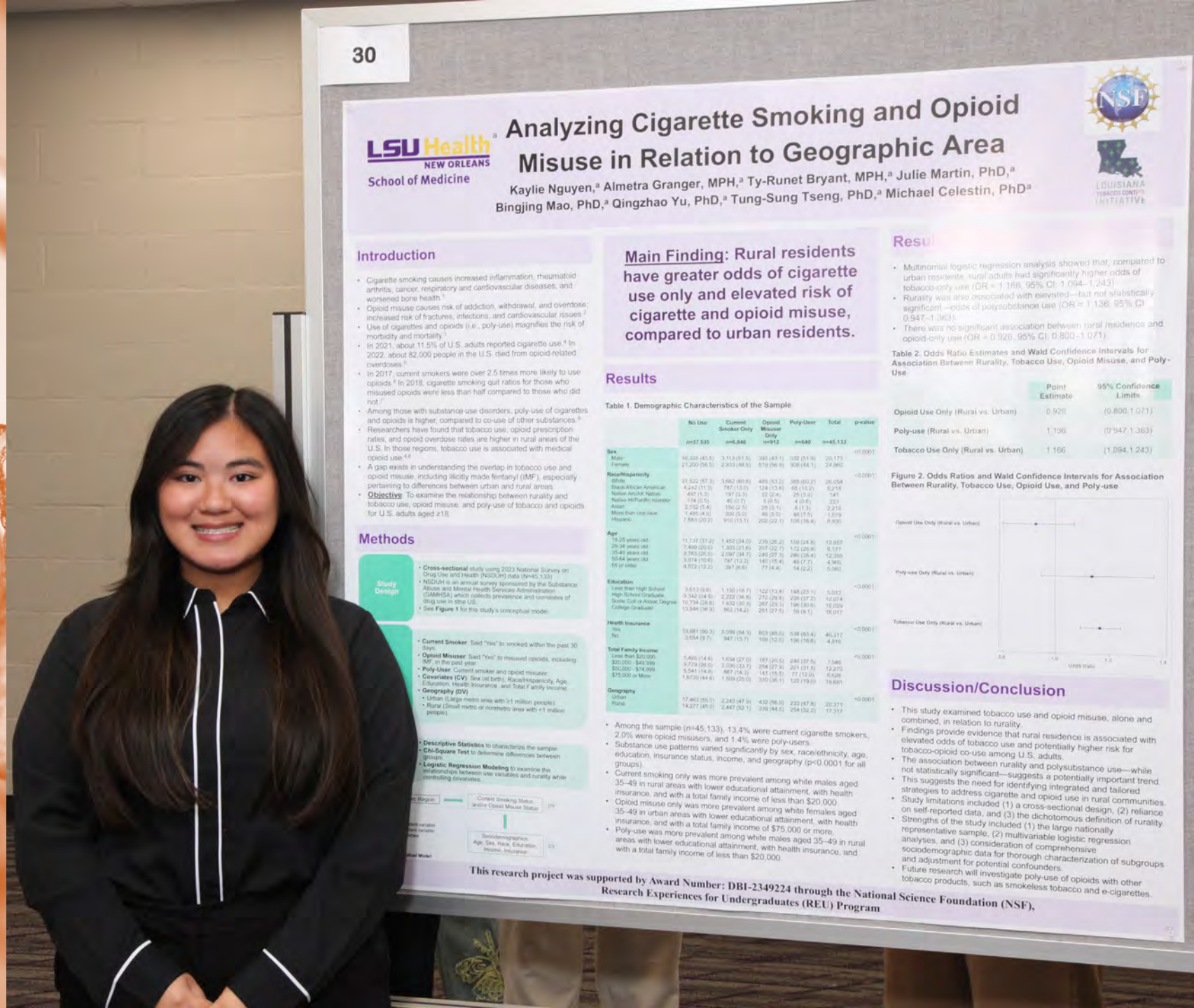
30
LSU Health NEW ORLEANS School of Medicine
Analyzing Cigarette Smoking and Opioid Misuse in Relation to Geographic Area
Kaylie Nguyen,[a] Almetra Granger, MPH,[a] Ty-Runet Bryant, MPH,[a] Julie Martin, PhD,[a]
Bingjing Mao, PhD,[a] Qingzhao Yu, PhD,[a] Tung-Sung Tseng, PhD,[a] Michael Celestin, PhD[a]
NSF
LOUISIANA TOBACCO CONTROL INITIATIVE
Introduction
Cigarette smoking causes increased inflammation, rheumatoid arthritis, cancer, respiratory and cardiovascular diseases, and worsened bone health.[1]
Opioid misuse causes risk of addiction, withdrawal, and overdose; increased risk of fractures, infections, and cardiovascular issues.[2]
Use of cigarettes and opioids (i.e., poly-use) magnifies the risk of morbidity and mortality.[3]
In 2021, about 11.5% of U.S. adults reported cigarette use.[4] In 2022, about 82,000 people in the U.S. died from opioid-related overdoses.[5]
In 2017, current smokers were over 2.5 times more likely to use opioids.[6] In 2018, cigarette smoking quit ratios for those who misused opioids were less than half compared to those who did not.[7]
Among those with substance use disorders, poly-use of cigarettes and opioids is higher, compared to co-use of other substances.[8]
Researchers have found that tobacco use, opioid prescription rates, and opioid overdose rates are higher in rural areas of the U.S. In those regions, tobacco use is associated with medical opioid use.[4,6]
A gap exists in understanding the overlap in tobacco use and opioid misuse, including illicitly made fentanyl (IMF), especially pertaining to differences between urban and rural areas.
Objective: To examine the relationship between rurality and tobacco use, opioid misuse, and poly-use of tobacco and opioids for U.S. adults aged ≥18.
Methods
Study Design
Cross-sectional study using 2023 National Survey on Drug Use and Health (NSDUH) data (N=45,133)
NSDUH is an annual survey sponsored by the Substance Abuse and Mental Health Services Administration (SAMHSA) which collects prevalence and correlates of drug use in the US.
See Figure 1 for this study's conceptual model.
Current Smoker: Said "Yes" to smoked within the past 30 days.
Opioid Misuser: Said "Yes" to misused opioids, including IMF, in the past year.
Poly-User: Current smoker and opioid misuser.
Covariates (CV): Sex (at birth), Race/Hispanicity, Age, Education, Health Insurance, and Total Family Income.
Geography (DV)
Urban (Large metro area with ≥1 million people)
Rural (Small metro or nonmetro area with <1 million people)
Descriptive Statistics to characterize the sample.
Chi-Square Test to determine differences between groups.
Logistic Regression Modeling to examine the relationships between use variables and rurality while controlling covariates.
Current Smoking Status and/or Opioid Misuse Status
DV
Sociodemographics: Age, Sex, Race, Education, Income, Insurance
CV
Main Finding: Rural residents have greater odds of cigarette use only and elevated risk of cigarette and opioid misuse, compared to urban residents.
Results
Table 1. Demographic Characteristics of the Sample
No Use n=37,535
Current Smoker Only n=6,046
Opioid Misuser Only n=912
Poly-User n=640
Total n=45,133
p-value
Sex
Male
Female
<0.0001
Race/Hispanicity
White
Black/African American
Native American/AK Native
Native HI/Pacific Islander
Asian
More than one race
Hispanic
<0.0001
Age
18-25 years old
26-34 years old
35-49 years old
50-64 years old
65 or older
<0.0001
Education
Less than High School
High School Graduate
Some Coll or Assoc Degree
College Graduate
<0.0001
Health Insurance
Yes
No
<0.0001
Total Family Income
Less than $20,000
$20,000 - $49,999
$50,000 - $74,999
$75,000 or More
<0.0001
Geography
Urban
Rural
<0.0001
Among the sample (n=45,133), 13.4% were current cigarette smokers, 2.0% were opioid misusers, and 1.4% were poly-users.
Substance use patterns varied significantly by sex, race/ethnicity, age, education, insurance status, income, and geography (p<0.0001 for all groups).
Current smoking only was more prevalent among white males aged 35–49 in rural areas with lower educational attainment, with health insurance, and with a total family income of less than $20,000.
Opioid misuse only was more prevalent among white females aged 35–49 in urban areas with lower educational attainment, with health insurance, and with a total family income of $75,000 or more.
Poly-use was more prevalent among white males aged 35–49 in rural areas with lower educational attainment, with health insurance, and with a total family income of less than $20,000.
Resul
Multinomial logistic regression analysis showed that, compared to urban residents, rural adults had significantly higher odds of tobacco-only use (OR = 1.166, 95% CI: 1.094–1.243).
Rurality was also associated with elevated—but not statistically significant—odds of polysubstance use (OR = 1.136; 95% CI: 0.947–1.363).
There was no significant association between rural residence and opioid-only use (OR = 0.926, 95% CI: 0.800–1.071).
Table 2. Odds Ratio Estimates and Wald Confidence Intervals for Association Between Rurality, Tobacco Use, Opioid Misuse, and Poly-Use
Point Estimate
95% Confidence Limits
Opioid Use Only (Rural vs. Urban)
0.926
(0.800,1.071)
Poly-use (Rural vs. Urban)
1.136
(0.947,1.363)
Tobacco Use Only (Rural vs. Urban)
1.166
(1.094,1.243)
Figure 2. Odds Ratios and Wald Confidence Intervals for Association Between Rurality, Tobacco Use, Opioid Use, and Poly-use
Opioid Use Only (Rural vs. Urban)
Poly-use Only (Rural vs. Urban)
Tobacco Use Only (Rural vs. Urban)
Discussion/Conclusion
This study examined tobacco use and opioid misuse, alone and combined, in relation to rurality.
Findings provide evidence that rural residence is associated with elevated odds of tobacco use and potentially higher risk for tobacco-opioid co-use among U.S. adults.
The association between rurality and polysubstance use—while not statistically significant—suggests a potentially important trend.
This suggests the need for identifying integrated and tailored strategies to address cigarette and opioid use in rural communities.
Study limitations included (1) a cross-sectional design, (2) reliance on self-reported data, and (3) the dichotomous definition of rurality.
Strengths of the study included (1) the large nationally representative sample, (2) multivariable logistic regression analyses, and (3) consideration of comprehensive sociodemographic data for thorough characterization of subgroups and adjustment for potential confounders.
Future research will investigate poly-use of opioids with other tobacco products, such as smokeless tobacco and e-cigarettes.
This research project was supported by Award Number: DBI-2349224 through the National Science Foundation (NSF), Research Experiences for Undergraduates (REU) Program

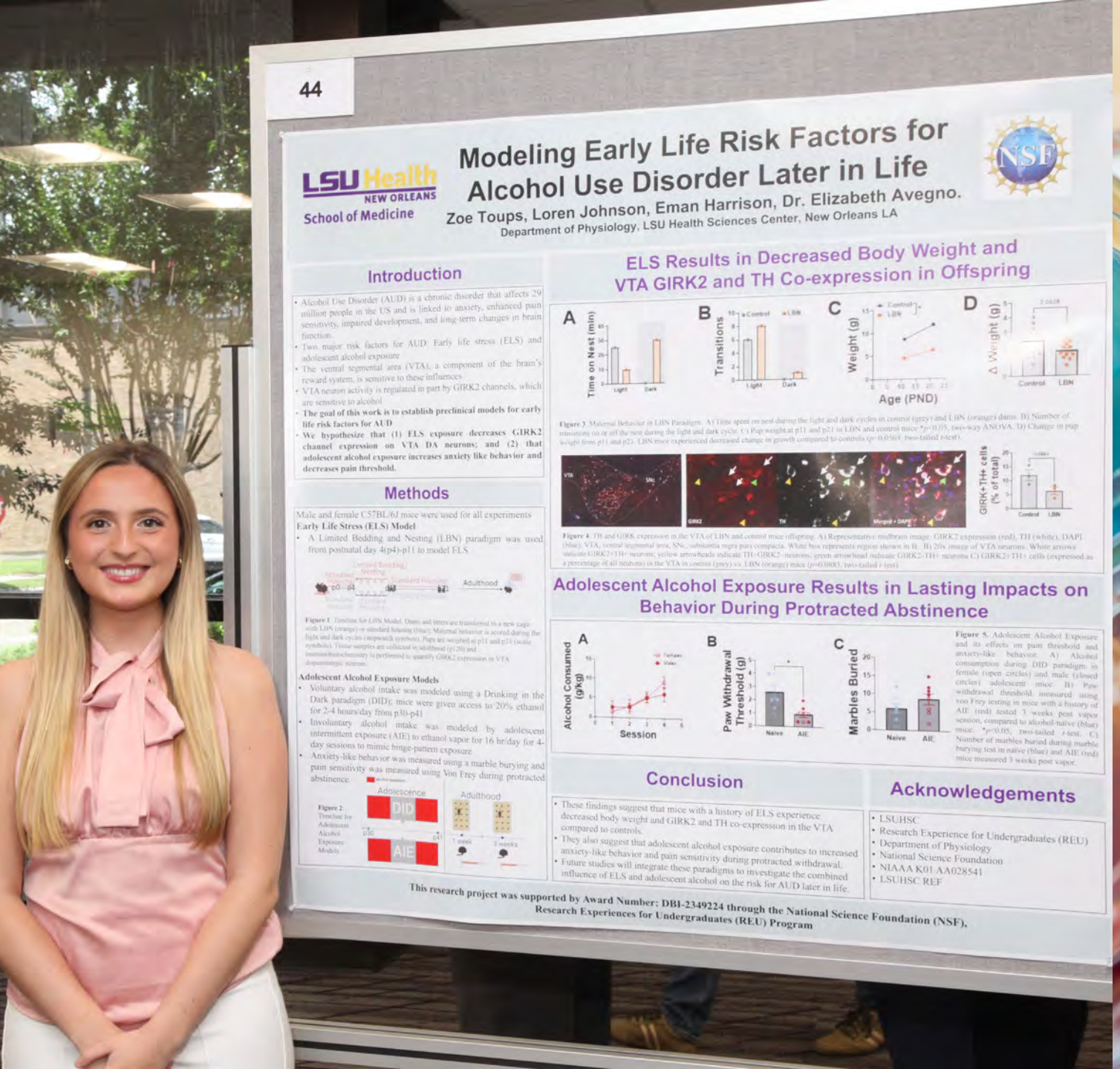

44

Modeling Early Life Risk Factors for Alcohol Use Disorder Later in Life

LSU Health NEW ORLEANS School of Medicine

Zoe Toups, Loren Johnson, Eman Harrison, Dr. Elizabeth Avegno.

Department of Physiology, LSU Health Sciences Center, New Orleans LA

Introduction

- Alcohol Use Disorder (AUD) is a chronic disorder that affects 29 million people in the US and is linked to anxiety, enhanced pain sensitivity, impaired development, and long-term changes in brain function.
- Two major risk factors for AUD: Early life stress (ELS) and adolescent alcohol exposure
- The ventral tegmental area (VTA), a component of the brain's reward system, is sensitive to these influences
- VTA neuron activity is regulated in part by GIRK2 channels, which are sensitive to alcohol
- **The goal of this work is to establish preclinical models for early life risk factors for AUD**
- **We hypothesize that (1) ELS exposure decreases GIRK2 channel expression on VTA DA neurons; and (2) that adolescent alcohol exposure increases anxiety like behavior and decreases pain threshold.**

Methods

Male and female C57BL/6J mice were used for all experiments

Early Life Stress (ELS) Model

- A Limited Bedding and Nesting (LBN) paradigm was used from postnatal day 4(p4)-p11 to model ELS

Figure 1. Timeline for LBN Model. Dams and litters are transferred to a new cage with LBN (orange) or standard housing (blue). Maternal behavior is scored during the light and dark cycles (stopwatch symbols). Pups are weighed at p11 and p21 (scale symbols). Tissue samples are collected in adulthood (p120) and immunohistochemistry is performed to quantify GIRK2 expression in VTA dopaminergic neurons.

Adolescent Alcohol Exposure Models

- Voluntary alcohol intake was modeled using a Drinking in the Dark paradigm (DID); mice were given access to 20% ethanol for 2-4 hours/day from p30-p41
- Involuntary alcohol intake was modeled by adolescent intermittent exposure (AIE) to ethanol vapor for 16 hr/day for 4-day sessions to mimic binge-pattern exposure
- Anxiety-like behavior was measured using a marble burying and pain sensitivity was measured using Von Frey during protracted abstinence.

Figure 2. Timeline for Adolescent Alcohol Exposure Models

ELS Results in Decreased Body Weight and VTA GIRK2 and TH Co-expression in Offspring

Figure 3. Maternal Behavior in LBN Paradigm. A) Time spent on nest during the light and dark cycles in control (grey) and LBN (orange) dams. B) Number of transitions on or off the nest during the light and dark cycle. C) Pup weight at p11 and p21 in LBN and control mice. *$p<0.05$, two-way ANOVA. D) Change in pup weight from p11 and p21. LBN mice experienced decreased change in growth compared to controls ($p=0.0503$, two-tailed t-test).

Figure 4. TH and GIRK expression in the VTA of LBN and control mice offspring. A) Representative midbrain image. GIRK2 expression (red), TH (white), DAPI (blue). VTA, ventral tegmental area; SNc, substantia nigra pars compacta. White box represents region shown in B. B) 20x image of VTA neurons. White arrows indicate GIRK2+TH+ neurons; yellow arrowheads indicate TH+GIRK2- neurons; green arrowhead indicate GIRK2+TH+ neurons C) GIRK2+TH+ cells (expressed as a percentage of all neurons) in the VTA in control (grey) vs. LBN (orange) mice ($p=0.0883$, two-tailed t-test).

Adolescent Alcohol Exposure Results in Lasting Impacts on Behavior During Protracted Abstinence

Figure 5. Adolescent Alcohol Exposure and its effects on pain threshold and anxiety-like behavior. A) Alcohol consumption during DID paradigm in female (open circles) and male (closed circles) adolescent mice. B) Paw withdrawal threshold, measured using von Frey testing in mice with a history of AIE (red) tested 3 weeks post vapor session, compared to alcohol-naïve (blue) mice. *$p<0.05$, two-tailed t-test. C) Number of marbles buried during marble burying test in naïve (blue) and AIE (red) mice measured 3 weeks post vapor.

Conclusion

- These findings suggest that mice with a history of ELS experience decreased body weight and GIRK2 and TH co-expression in the VTA compared to controls.
- They also suggest that adolescent alcohol exposure contributes to increased anxiety-like behavior and pain sensitivity during protracted withdrawal.
- Future studies will integrate these paradigms to investigate the combined influence of ELS and adolescent alcohol on the risk for AUD later in life.

Acknowledgements

- LSUHSC
- Research Experience for Undergraduates (REU)
- Department of Physiology
- National Science Foundation
- NIAAA K01 AA028541
- LSUHSC REF

This research project was supported by Award Number: DBI-2349224 through the National Science Foundation (NSF), Research Experiences for Undergraduates (REU) Program

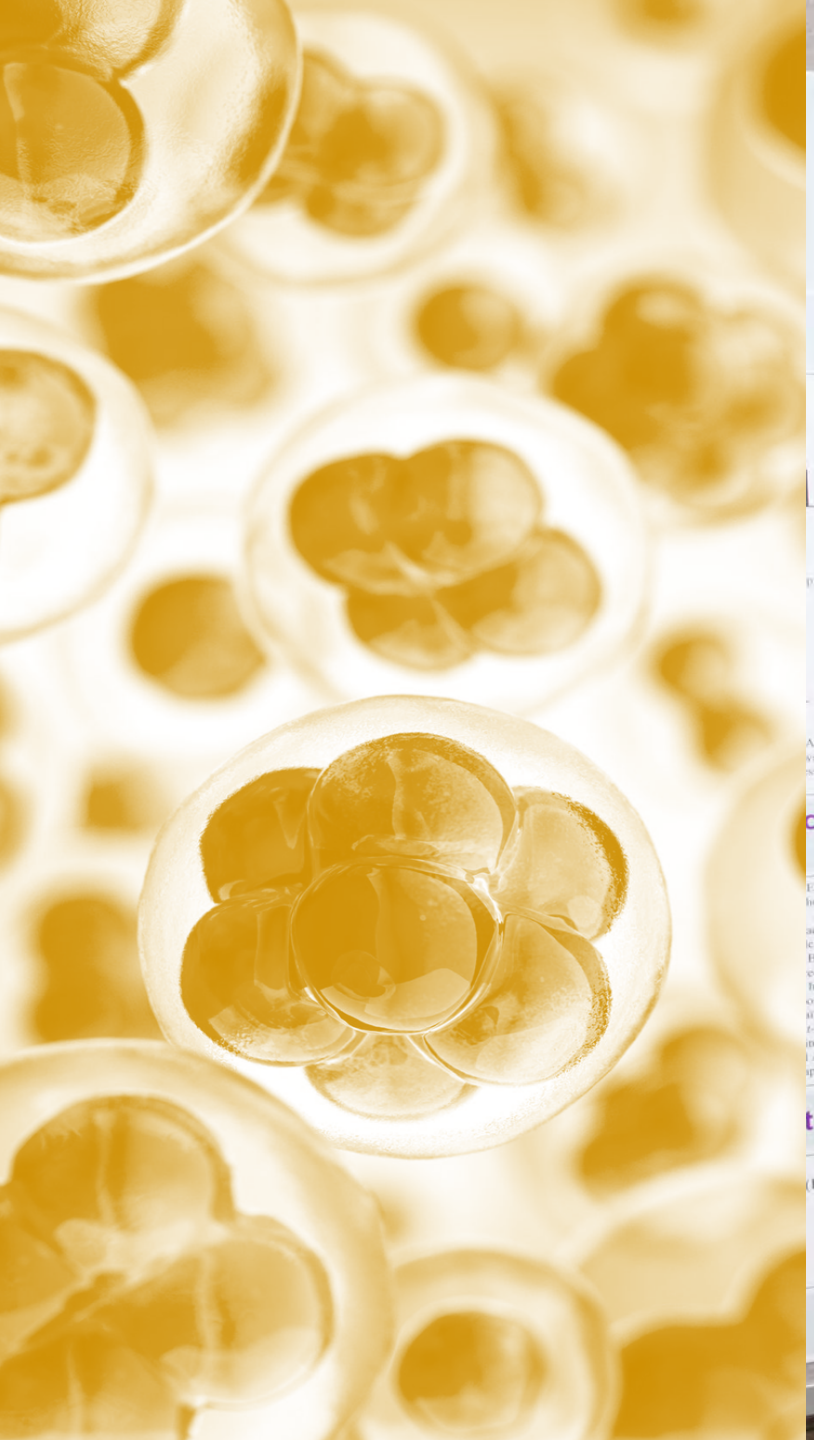

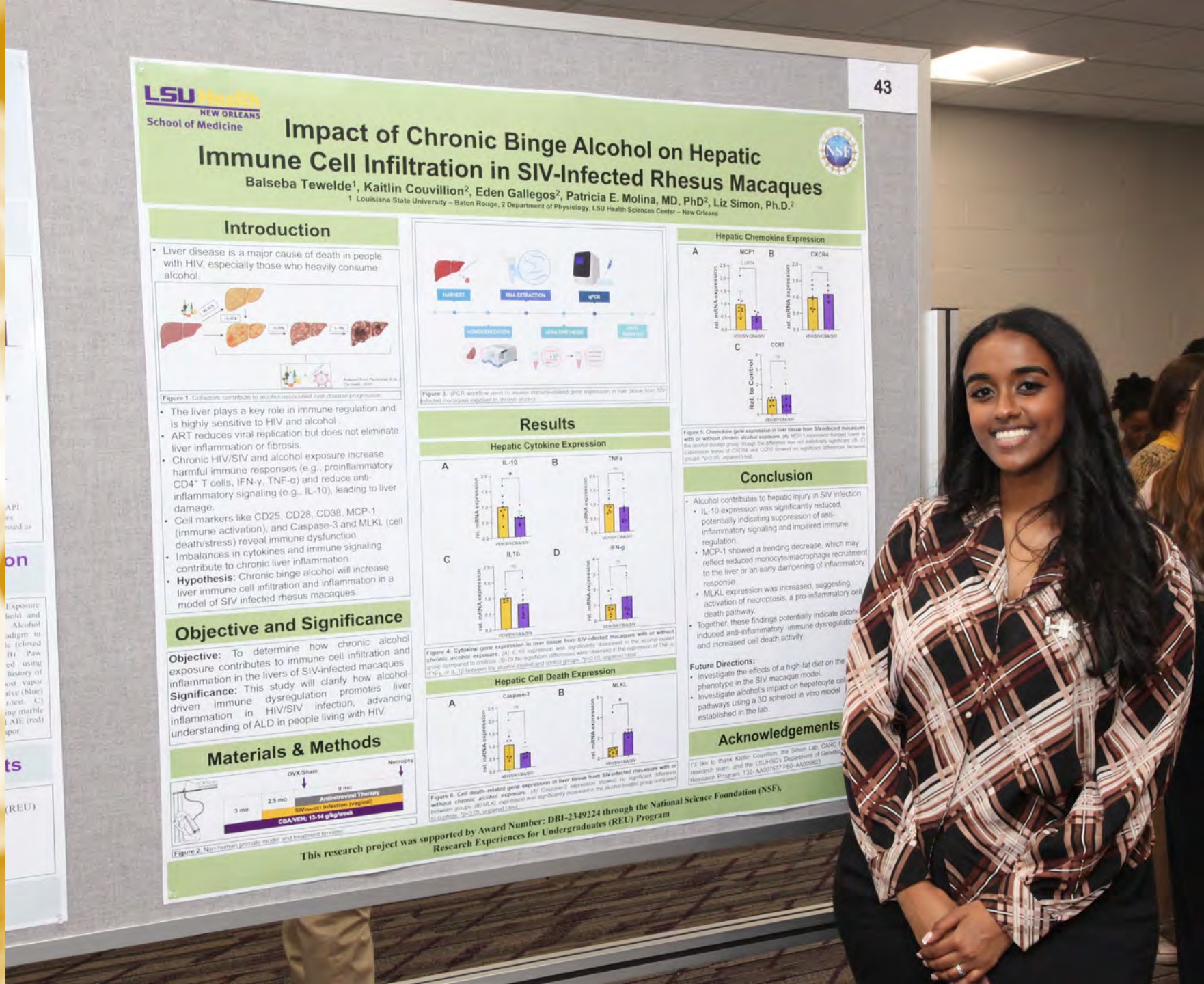

LSU Health NEW ORLEANS School of Medicine

Impact of Chronic Binge Alcohol on Hepatic Immune Cell Infiltration in SIV-Infected Rhesus Macaques

Balseba Tewelde[1], Kaitlin Couvillion[2], Eden Gallegos[2], Patricia E. Molina, MD, PhD[2], Liz Simon, Ph.D.[2]
1 Louisiana State University – Baton Rouge, 2 Department of Physiology, LSU Health Sciences Center – New Orleans

Introduction

- Liver disease is a major cause of death in people with HIV, especially those who heavily consume alcohol.

Figure 1. Cofactors contribute to alcohol-associated liver disease progression.

- The liver plays a key role in immune regulation and is highly sensitive to HIV and alcohol.
- ART reduces viral replication but does not eliminate liver inflammation or fibrosis.
- Chronic HIV/SIV and alcohol exposure increase harmful immune responses (e.g., proinflammatory $CD4^+$ T cells, IFN-γ, TNF-α) and reduce anti-inflammatory signaling (e.g., IL-10), leading to liver damage.
- Cell markers like CD25, CD28, CD38, MCP-1 (immune activation), and Caspase-3 and MLKL (cell death/stress) reveal immune dysfunction.
- Imbalances in cytokines and immune signaling contribute to chronic liver inflammation.
- **Hypothesis**: Chronic binge alcohol will increase liver immune cell infiltration and inflammation in a model of SIV infected rhesus macaques.

Objective and Significance

Objective: To determine how chronic alcohol exposure contributes to immune cell infiltration and inflammation in the livers of SIV-infected macaques.

Significance: This study will clarify how alcohol-driven immune dysregulation promotes liver inflammation in HIV/SIV infection, advancing understanding of ALD in people living with HIV.

Materials & Methods

Figure 3. qPCR workflow used to assess immune-related gene expression in liver tissue from SIV-infected macaques exposed to chronic alcohol.

Figure 2. Non-human primate model and treatment timeline.

Results

Hepatic Cytokine Expression

Figure 4. Cytokine gene expression in liver tissue from SIV-infected macaques with or without chronic alcohol exposure. (A) IL-10 expression was significantly decreased in the alcohol-treated group compared to controls. (B–D) No significant differences were observed in the expression of TNF-α, IFN-γ, or IL-1β between the alcohol-treated and control groups. *p<0.05, unpaired t-test.

Hepatic Cell Death Expression

Figure 6. Cell death-related gene expression in liver tissue from SIV-infected macaques with or without chronic alcohol exposure. (A) Caspase-3 expression showed no significant difference between groups. (B) MLKL expression was significantly increased in the alcohol-treated group compared to controls. *p<0.05, unpaired t-test.

Hepatic Chemokine Expression

Figure 5. Chemokine gene expression in liver tissue from SIV-infected macaques with or without chronic alcohol exposure. (A) MCP-1 expression trended lower in the alcohol-treated group, though the difference was not statistically significant. (B, C) Expression levels of CXCR4 and CCR5 showed no significant differences between groups. *p<0.05, unpaired t-test.

Conclusion

- Alcohol contributes to hepatic injury in SIV infection.
  - IL-10 expression was significantly reduced, potentially indicating suppression of anti-inflammatory signaling and impaired immune regulation.
  - MCP-1 showed a trending decrease, which may reflect reduced monocyte/macrophage recruitment to the liver or an early dampening of inflammatory response.
  - MLKL expression was increased, suggesting activation of necroptosis, a pro-inflammatory cell death pathway.
- Together, these findings potentially indicate alcohol-induced anti-inflammatory immune dysregulation and increased cell death activity.

Future Directions:

- Investigate the effects of a high-fat diet on the phenotype in the SIV macaque model.
- Investigate alcohol's impact on hepatocyte cell pathways using a 3D spheroid in vitro model established in the lab.

Acknowledgements

I'd like to thank Kaitlin Couvillion, the Simon Lab, CARC f... research team, and the LSUHSC's Department of Genetics... Research Program. T32- AA007577 P60- AA009803

This research project was supported by Award Number: DBI-2349224 through the National Science Foundation (NSF), Research Experiences for Undergraduates (REU) Program

43